



Cite this: *Chem. Commun.*, 2025, 61, 1303

Received 29th September 2024,  
Accepted 6th December 2024

DOI: 10.1039/d4cc05078a

rsc.li/chemcomm

# Catalytic conversion of chitin biomass into key platform chemicals

Xinlei Ji,  Yichang Lu and Xi Chen  \*

Chitin is the most abundant nitrogen-containing biomass on Earth and presents a compelling alternative to fossil fuels for chemical production. The catalytic conversion of chitin offers a viable approach for harnessing its inherent carbon and nitrogen contents, contributing to developing a green and sustainable society. This feature article reviews recent advances in shell waste biorefinery, with an emphasis on the contributions from our group. Efficient and sustainable chitin extraction methods are highlighted, along with the conversion of chitin biomass (*N*-acetyl-D-glucosamine (NAG), D-glucosamine, chitosan, and chitin) into key platform chemicals, mainly including furans, amino/amide sugars, organic acids and amino/amide acids. Catalytic strategies and production pathways are detailed, and current challenges and future research directions in chitin valorization are discussed.

## Introduction

The excessive consumption of nonrenewable fossil fuels has given rise to significant environmental and economic challenges, such as global warming, energy crises, and the depletion of natural resources.<sup>1–6</sup> Consequently, seeking renewable and sustainable alternatives has become an urgent necessity to address these issues and ensure the sustainable development of society.<sup>7–13</sup> Biomass resources are commonly regarded as one of the most ideal alternatives to fossil feedstocks, due to their renewable, abundant, widely available, and inexpensive nature.<sup>14–18</sup> Lignocellulose is the most abundant biomass resource on Earth, primarily composed of cellulose, hemicellulose, and lignin. As a rich and renewable source of chemicals,

the valorization of lignocellulosic biomass has been prevalently researched in the past decades.<sup>19–23</sup>

Currently, the spotlight in research has shifted from land-based biomass to ocean-based biomass. The shift towards ocean-based biomass is mainly driven by its potential to alleviate land area constraints, a critical issue in some countries.<sup>24</sup> Furthermore, ocean-based biomass requires less infrastructure, has faster growth rates, thrives under less demanding growth conditions, and contains numerous bioactive compounds that have yet to be fully explored. Chitin, the world's second most abundant biomass resource with an annual production exceeding 10<sup>5</sup> million metric tons,<sup>25</sup> is characterized by its linear and relatively homogeneous polymer structure, primarily composed of NAG monosaccharides, linked by  $\beta$ -(1,4)-glycosidic bonds.<sup>26,27</sup> It exists not only in crustacean shells (particularly marine organisms) but also in the skeletons of insects, various fungi, etc.<sup>28,29</sup> With its natural

China-UK Low Carbon College, Shanghai Jiao Tong University, 3 Yinlian Road, Shanghai, China. E-mail: chenxi-lcc@sjtu.edu.cn



Xinlei Ji

Xinlei Ji received her Bachelor's Degree from the China University of Petroleum (East China). She is currently a PhD student at Shanghai Jiao Tong University, under the supervision of Professor Xi Chen. Her research mainly focuses on biomass valorization into materials and chemicals.



Yichang Lu

Yichang Lu is a Master's student in Resources and Environment at Shanghai Jiao Tong University, under the supervision of Professor Xi Chen. Her research mainly focuses on the conversion of biomass waste into high value-added products.

nitrogen elements, chitin is an ideal raw material for producing nitrogen-containing compounds. Unlike lignocellulosic biomass, chitin enables the co-production of both nitrogenous and oxygenated platform chemicals, including furans, amino/amide sugars and amino/amide acids, thereby broadening the range of potential products. Besides, chitin offers a complementary pathway for the sustainable production of oxygen-containing chemicals such as acetic acid due to the presence of an acetamido side chain in its structure. In addition, compared to land-based biomass, chitin is ocean-based and occupies less land resources. As a key component of shell waste, chitin supports resource sustainability by providing an alternative feedstock that complements carbohydrate-based biomass and contributes to the circular economy.

The concept of shell biorefinery was recently proposed,<sup>30</sup> which encompasses the fractionation and transformation of various shells from crustacean species and insects into valuable oxygen- and nitrogen-containing chemicals. It offers sustainable, economically beneficial, and environmentally friendly solutions by utilizing waste shells, which reduces the carbon footprint and produces versatile high-value products for various industries.<sup>31–33</sup> In the current industrial practice, chitin is primarily extracted from crustacean shells (such as crabs and shrimp), whereas extraction from insects and fungi continues to pose significant challenges. The extraction of chitin is a fundamental prerequisite for virtually all biorefinery processes, and thus developing a green and sustainable fractionation method is essential. With chitin biomass as the resource, different transformation routes such as hydrolysis, dehydration, oxidation, *etc.* can be explored to obtain a series of value-added key platform chemicals (Fig. 1). Our research focus has been devoted to shell waste biorefinery in the past years, mainly including the production of furans, amino/amide sugars, organic acids and amino acids from chitin biomass. Meanwhile, endeavors have also been made to develop a greener and more economically feasible extraction method from shell waste. These relevant works will be briefly summarized in this feature article, and it is expected to provide useful information

and guidance for future studies in the field of waste shell biorefinery.

## The extraction of chitin from shell waste

To convert chitin biomass into valuable compounds, the important first step is to obtain/extract chitin from the shell waste (usually shrimp, crab or lobster shells). Generally, the waste shell is composed of three major components including proteins (20–40%), calcium carbonate (20–50%) and chitin (15–40%).<sup>34</sup> These three components were entangled tightly with each other in the shell, which poses challenges for fractionation/extraction. The current industrial extraction method is fraught with significant environmental and economic concerns, which is one of the major reasons that most of the shell waste generated annually (as an estimated amount of 4–5 million tons) is directly dumped or landfilled without further utilization.<sup>35</sup> The industrial method normally employs strong acids (*e.g.* HCl) and bases (*e.g.* NaOH) to peel off the minerals and proteins, respectively, causing great problems of high capital costs, high environmental burdens and restricted management.<sup>36–38</sup> Emerging methods have been explored such as the solvent method and the bioprocessing method. The solvent extraction method, such as those using ionic liquids (ILs), offers a promising alternative but is hampered by high costs and difficulties in solvent recovery.<sup>39–41</sup> The bioprocessing method, which utilizes enzymes or microorganisms, results in low product purity and prolonged processing times.<sup>42–44</sup> These challenges could lead to the high price of extracted chitin, thereby impacting the market competitiveness.

To address these challenges, our group developed the HOW-CA process, a novel fractionation technique that utilizes only hot water and carbonic acid as environmentally benign reagents for deproteinization and demineralization on waste shells (shrimp shell powders were used as the demonstration) to produce high-purity chitin.<sup>45</sup> The whole process is shown in Fig. 2a. In the first step, shrimp shell powders were treated with hot water at 180 °C, where the protons and hydroxide ions generated from the subcritical water promoted nearly full dissolution of proteins and catalyzed the partial hydrolysis of proteins. With the removal of proteins, the minerals in the residue, primarily calcium carbonate (CaCO<sub>3</sub>), were adequately exposed. The residue was then subjected to pressurized carbon dioxide (CO<sub>2</sub>) in an aqueous solution for demineralization. The weak acidity of CO<sub>2</sub> dissolved in water decomposed CaCO<sub>3</sub> into soluble calcium bicarbonate, achieving nearly 100% demineralization under 10 bar CO<sub>2</sub> pressure at room temperature. Both water and CO<sub>2</sub> could be recycled in this process. CaCO<sub>3</sub> reprecipitated from the water during CO<sub>2</sub> release (pressure drop) could be recovered as a useful by-product. The entire HOW-CA process could be completed within hours, yielding high-purity chitin (>90%), with the crystalline structure well preserved. The final product exhibited similar crystallinity index values and infrared spectroscopy (IR) spectra as commercial chitin and retained the typical fibrous structure of chitin



Xi Chen

*Xi Chen received her Bachelor (2010) and Master (2012) degrees from Wuhan University in China. She then obtained her PhD degree in Chemical Engineering from the National University of Singapore (NUS) under the supervision of Prof. Ning Yan in 2016, where she stayed as a postdoc. She joined the China-UK Low Carbon College at Shanghai Jiao Tong University in 2018 and is now an Associate Professor. Her group focuses on the chemical utilizations of various waste resources including biomass, plastics and CO<sub>2</sub>.*

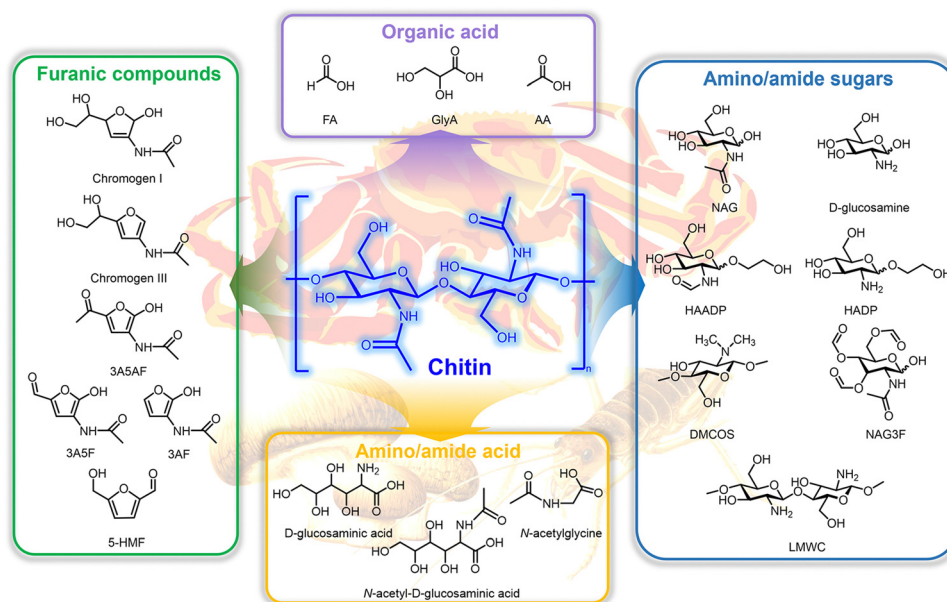


Fig. 1 Key platform chemicals via the catalytic conversion of chitin.

extracted using conventional methods. As a result, the HOW-CA process demonstrated comparable performance for chitin fractionation to the existing methods but boasted unique advantages. Moreover, this process was applicable to scale-up production. As presented in Fig. 2b, starting with 25 g of shrimp shells, 95.3% deproteinization efficiency was achieved at 180 °C for 1 h in a high loading of 0.1 g mL<sup>-1</sup>. Subsequently, three cycles of demineralization removed >90% of minerals. To evaluate the scalability and economic feasibility of the HOW-CA process, process modeling was conducted using Aspen Plus V10 based on a shrimp shell treatment rate of 100 kg h<sup>-1</sup>. Compared to the traditional method, which uses harsh chemicals like NaOH and HCl, the use of water and CO<sub>2</sub> as low-cost reagents in the HOW-CA process not only reduces total operating costs but also simplifies the process design for easier scaling-up. Economically, the HOW-CA process achieves a significantly lower minimum selling price (9.9 USD per kg), reducing it by more than half compared to the traditional method. Sensitivity analysis also demonstrated that the HOW-CA process is less sensitive to fluctuations in operating costs, which offers greater stability for large-scale industrial applications. Furthermore, life-cycle analysis suggested that HOW-CA is a superior alternative to the conventional method, offering a cost-effective and environmentally friendly solution for extracting high-value chitin from crustacean shells.

Recent studies have explored the use of deep eutectic solvents (DESs) as a greener alternative to traditional methods for extracting chitin.<sup>46–49</sup> DESs, composed of hydrogen bond donors (HBDs) and hydrogen bond acceptors (HBAs), are non-toxic and biodegradable and have adjustable solvation properties.<sup>50</sup> In the extraction process, DESs release protons to dissolve CaCO<sub>3</sub>, weakening the chitin–protein fibrils and allowing them to be separated. Proteins, which possess active functional groups like hydroxyl, carboxyl and amine groups,

form new hydrogen bonds with the DES's HBAs, further aiding in their separation.<sup>51</sup>

Various DESs have been successfully applied to extract chitin from different raw materials.<sup>51–55</sup> For instance, ChCl-based DESs, including mixtures of ChCl with organic acids like citric acid or malic acid, are particularly effective due to their low costs and strong solvating ability. Chitin extracted from shrimp shells using ChCl/malic acid with different compositions has shown yields ranging from 13.1% to 56.6%, with purity between 89.9% and 93.4%.<sup>54</sup> Similarly, extraction from lobster shells using ChCl/malonic acid has obtained chitin with a yield of 19.6% to 23.3% and purity ranging from 90% to 93%.<sup>55</sup> In contrast, chitin extracted from insect sources like *Hermetia illucens* tends to have a lower yield (6.5% to 26.7%) and purity (74.7% to 91.3%) due to the lower chitin content in insect exoskeletons.<sup>52</sup> Besides, the yield and purity of chitin are influenced by the properties and compositions of DESs, including the pH, HBA/HBD ratio, water content, *etc.* Acidic DESs, particularly those containing ChCl, are more efficient at breaking down minerals and proteins, thereby improving purity but often resulting in lower yields compared to betaine-based DESs.<sup>52</sup> A lower ratio of HBAs to HBDs increases the acidity of the DES, enhancing demineralization and deproteinization, but this can lead to a reduction in the chitin yield.<sup>54</sup> Additionally, adding water to the DES can improve demineralization efficiency and assist in the precipitation of dissolved chitin, which can improve the recovery process.<sup>51,53</sup>

In conclusion, while DESs offer a promising, eco-friendly alternative for chitin extraction, future research should focus on optimizing these parameters to maximize both yield and purity. Further investigations into new DES formulations, as well as strategies to improve the recycling and reusability of DESs, are essential for making the extraction process more sustainable and cost-effective.



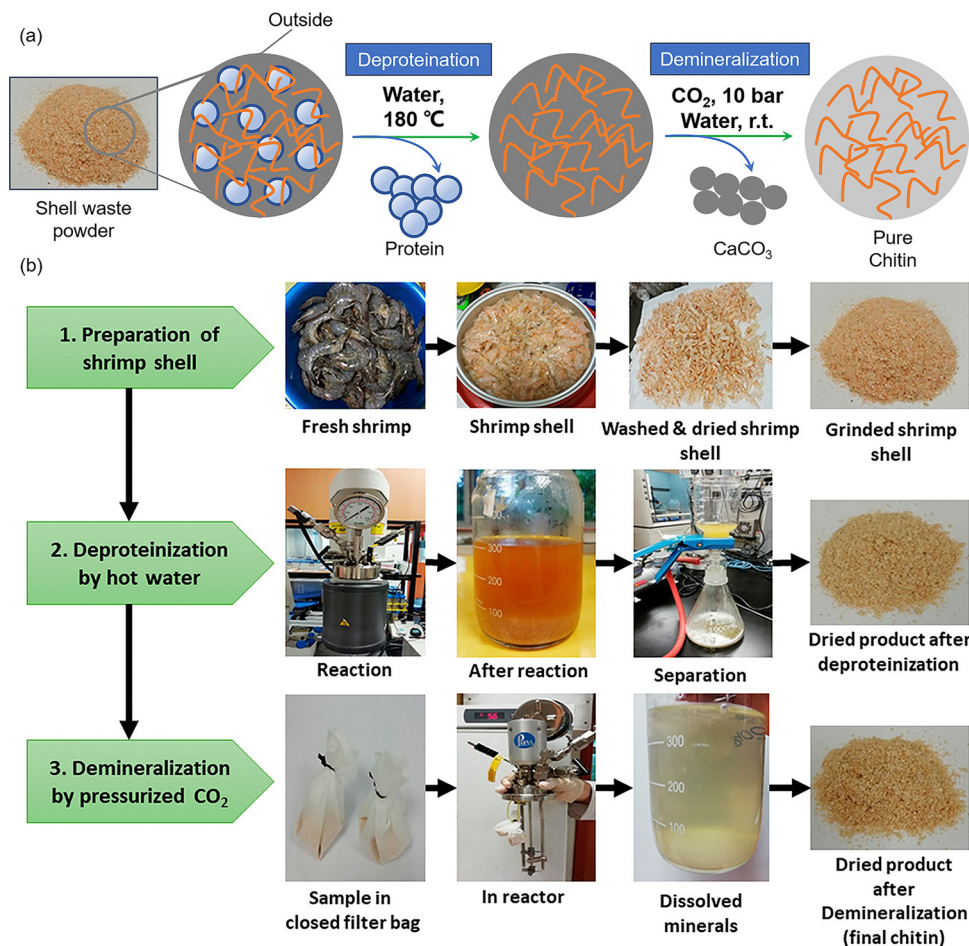


Fig. 2 (a) The schematic diagram of the HOWCA process. (b) Images of processes involved in the HOW-CA process starting with 25 g of raw shrimp shells. Reproduced from ref. 45 with permission from American Chemical Society, copyright 2019.

## Furanic platform compounds

Furanic compounds represent a variety of versatile building blocks that possess the furan ring which could be derived from several biomass resources such as chitin biomass. Especially, 3-acetamido-5-acetylfuran (3A5AF) is a unique platform molecule derived from chitin dehydration. It boasts a distinctive structure featuring a furan ring with an acetamido group at position 3 and an acetyl group at position 5. This molecule is notable for its biologically fixed nitrogen with the potential as a sustainable and renewable building block in chemical synthesis.<sup>56–59</sup> Such a substitution structure is relatively difficult to access through the classical organic synthesis methods, whereas direct conversion of chitin into 3A5AF could be more efficient, renewable and selective. 3A5AF can be further upgraded into valuable derivatives, such as biomedical, pharmaceuticals and dyes, with applications in pharmaceuticals, agrochemicals and materials science. For example, various nitrogen-containing downstream products, including 2-acetyl-4-aminofuran, 3-acetamido-5-(1-hydroxyethyl)furan, 7-oxanorbornenes, and dihydrodifluoropyridine, can be synthesized from 3A5AF through processes like hydrolysis, reduction, Diels–Alder reactions and electrophilic halogenation.<sup>56–61</sup> These products are vital in numerous

industries, and the upgrading of 3A5AF offers a more sustainable alternative to conventional synthesis methods that rely on non-renewable fossil fuels. Our previous works demonstrated the advantages of using chitin as a resource for synthesizing the anticancer alkaloid proximicin A, which benefited from a shortened reaction pathway and the use of greener reagents compared to fossil-based routes<sup>62</sup> (Fig. 3).

The selective production of 3A5AF from the chitin monomer NAG was first achieved by Kerton's group using microwave irradiation at a temperature window of 180–220 °C. It was unraveled that boric acid played a crucial role in promoting NAG dehydration in 1-butyl-3-methylimidazolium chloride ([BMIm]Cl) ILs or dimethylformamide (DMA) solvent.<sup>63,64</sup> The 3A5AF yield could reach >60% under optimal conditions. Our group has reported the direct conversion of chitin polymers into 3A5AF based on the catalytic system with boric acid, alkaline chloride and mineral acid as combinational promoters, with an emphasis on the reaction pathway and the mechanism.<sup>65</sup> A variety of side products such as oligomers, aromatics and organic acids have been probed by different analytical techniques, which assisted the assumption of the reaction pathways. Several parallel reaction pathways have been identified and proposed (Fig. 4). Chitin depolymerization was

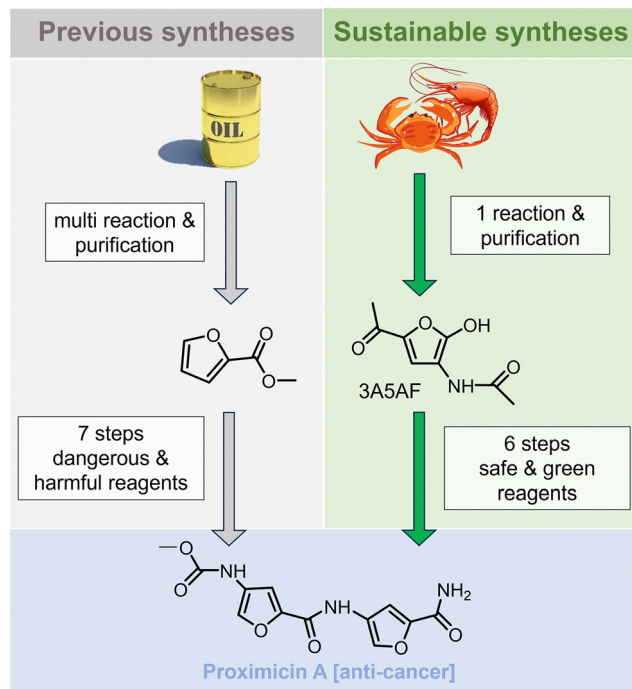


Fig. 3 The comparison of proximicin A synthesis from fossil and chitin resources.

regarded as the first step to afford oligomers and NAG, then the ring-opening of the pyranose, the reformation of the furan ring and dehydration occurred to produce 3A5AF. Meanwhile, deacetylation occurred leading to side products including acetic acid, levoglucosenone and a polymeric solid known as chitin-humins. Another side route (ring arrangement and dehydration) would result in the formation of the 4-(acetylamino)-1,3-benzenediol side product. To further elucidate the unique role of boric acid on dehydration, poisoning tests and nuclear magnetic resonance (NMR) studies have been employed. The addition of ethylene glycol and 1,3-propanediol as the poison reagent has led to a significant drop in the 3A5AF yield, suggesting that the boric acid possibly interacted with two hydroxyl groups of chitin to promote dehydration. Combined with the  $^1\text{H}$ ,  $^{11}\text{B}$  and  $^{13}\text{C}$  NMR analyses, the signals assigned to the proton of two hydroxyl groups disappeared upon boric acid addition on the  $^1\text{H}$  NMR spectra, while a new peak appeared on the  $^{11}\text{B}$  NMR spectra. Besides, new groups of peaks and peak shifts have been observed on the  $^{13}\text{C}$  NMR spectra, which indicated the formation of the boron-NAG complex through the coordination at the two sites of C4 and C6 positions. Boric acid has formed such an intermediate with NAG and facilitated the ring-opening and subsequent dehydration.

Due to the high crystallinity, high molecular weight (MW) and extensive hydrogen bonds of chitin polymers, the direct conversion of chitin polymers into 3A5AF resulted in a relatively low yield of 7.5% in the NMP solvent at  $215^\circ\text{C}$  using boric acid, lithium chloride and HCl as the promoters.<sup>65</sup> Following this, we have investigated the performance of different ILs for direct chitin conversion.<sup>66</sup> Although several IL-containing chloride

anions would notably enhance chitin solubility and accelerate the initial reaction rate, the 3A5AF yield was not obviously improved despite the reaction temperature being lower at  $180^\circ\text{C}$ . We have also tried extraction and vacuum-distillation techniques to get the 3A5AF out from the solvent during the reaction, to drive the reaction equilibrium towards 3A5AF and increase the yield. However, such techniques were not effective because the product 3A5AF seemed to strongly interact with the [BMIm]Cl solvent and was very difficult to extract out. To promote the direct conversion of chitin polymers into 3A5AF, pretreatment has been adopted and proven as an efficient tool. Notably, effective pretreatment methods can disrupt the chitin's crystalline structure and hydrogen-bonding network. We have evaluated five pretreatment methods: ball mill grinding, steam explosion, alkaline treatment, phosphoric acid treatment and ionic liquid dissolution/precipitation.<sup>67</sup> Among these, ball mill grinding in dry mode was the most effective, significantly reducing the crystallinity and the hydrogen-bonding network. This approach increased the 3A5AF yield to 28.5% under milder conditions of  $180^\circ\text{C}$  within 10 min from 7.5% which was previously achieved at  $215^\circ\text{C}$  for 1 h. This study underscores the importance of structural modifications in enhancing chitin reactivity, with reduced crystal size and a weakened hydrogen-bonding network being key factors in improving conversion efficiency.

Along this line, other groups have developed different catalytic systems, including metal chlorides, ammonium salts, acidic chloride-ion based ionic liquids and DESs, for NAG dehydration. For metal chloride catalysts, Fukuoka's group has introduced a simplified method for 3A5AF production using  $\text{AlCl}_3 \cdot 6\text{H}_2\text{O}$  as the catalyst in the DMA solvent, with a peak yield of 30%.<sup>68</sup> This method operated effectively at a higher substrate-to-catalyst ratio and a reduced temperature of  $120^\circ\text{C}$ , successfully enabling the isolation of 3A5AF at the gram scale. The Zang group has developed several chlorine-based ionic liquid catalysts, including glycine chloride, 1-chloro-3-methylpyridinium chloride, triethylammonium chloride, 1-chloro-1-(3-hydroxypropyl)pyridinium chloride and pyrazole chloride, which achieved 3A5AF yields ranging from 43% to 70% at temperatures beyond  $180^\circ\text{C}$  in organic solvents.<sup>69–73</sup> Acidic ILs could promote dehydration by enhancing solubility and releasing protons, which aids the efficient process. Among these, pyrazole chloride showed the best performance, yielding 70% of 3A5AF when combined with boric acid and  $\text{CaCl}_2$  in DMA solvent.<sup>74</sup> Furthermore, Zhang and Chen's group demonstrated that ammonium salts are effective for chitin biomass dehydration.<sup>75,76</sup> Using NAG as the starting material, 3A5AF was obtained with a yield of 43% in the presence of  $\text{NH}_4\text{Cl}$  and  $\text{LiCl}$  in DMF.<sup>76</sup> For chitin dehydration, chitin was first enzymatically hydrolyzed to NAG, followed by chemical conversion to 3A5AF using  $\text{NH}_4\text{SCN}$  as the promoter, achieving a yield of 56.7% at  $180^\circ\text{C}$  in the DMA solvent.<sup>75</sup> The work has demonstrated a feasible method for 3A5AF separation and extraction. The reaction mixture was subjected to extraction with ethyl acetate, followed by evaporation for concentrations. The resulting residue underwent decolorization to eliminate impurities, and the product was crystallized to yield needle-shaped 3A5AF crystals with 99% purity. However, the overall process resulted in a yield loss

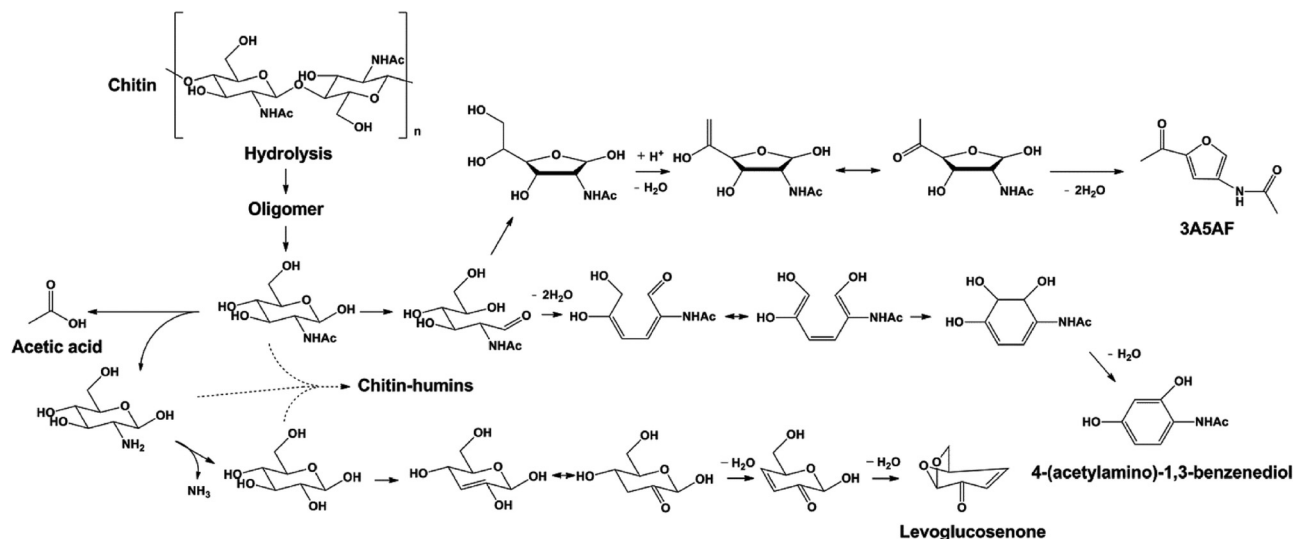


Fig. 4 Proposed parallel reaction pathway during the process of chitin conversion into 3A5AF with boric acid, lithium chloride and HCl as the promoters in the *N*-methyl-2-pyrrolidone (NMP) solvent. Reproduced from ref. 65 with permission from The Royal Society of Chemistry, copyright 2014.

compared to the initial conversion due to the extraction and purification steps. Future research could focus on optimizing the separation and purification steps to improve the overall yield and minimize losses during the process.

Recently, Wang and colleagues reported the use of choline chloride-based DESs for the selective production of either chromogen III or 3A5AF in the DMA solvent, achieving optimal yields of 31.1% and 39.2%, respectively.<sup>77</sup> In the presence of a binary DES (ChCl-Gly), chromogen III was the major product, whereas the use of a ternary DES (ChCl-Gly-B(OH)<sub>3</sub>) shifted the reaction pathway, favoring the formation of 3A5AF as the dominant product. This progress suggests that the combinational use of Brønsted and Lewis acids could be beneficial for 3A5AF formation. In addition, chloride or other anions with similar properties, such as the thiocyanate ion, is possibly necessary because it strongly interacts with the hydroxyl groups on NAG to disrupt the hydrogen-bonding network.

Unfortunately, although different catalytic systems have been explored, chitin dehydration to produce 3A5AF still employed highly toxic organic solvents or expensive ILs under relatively harsh conditions, which could not meet the demand for green synthesis and hindered practical applications. To address these issues, our group developed an environmentally friendly method that efficiently converted NAG into 3A5AF using the sustainable, non-toxic and biobased  $\gamma$ -valerolactone (GVL) solvent under milder conditions.<sup>78</sup> This method leveraged a dissolution-dehydration effect (Fig. 5a) that significantly enhanced the 3A5AF production, achieving an unprecedented yield of 75% using NH<sub>4</sub>SCN and HCl as the catalysts. Among the thirty different species of catalysts tested, including metal halides, ammonium salts, acids, *etc.*, NH<sub>4</sub>SCN has shown the highest performance in 3A5AF production in GVL (Fig. 5b). It was observed that NAG did not dissolve in GVL at room temperature or even when heated to a certain high temperature, but became almost completely dissolved upon the addition of NH<sub>4</sub>SCN (Fig. 5b). In addition,

NH<sub>4</sub>SCN coordinated with the acetamido and hydroxyl groups on NAG, accelerating its conversion to partially dehydrated intermediates, chromogens I and III, which subsequently underwent further dehydration to form 3A5AF. Notably, a high 3A5AF yield of over 70% was achieved within a relatively mild temperature range of 130–150 °C (Fig. 5c), considerably lower than the temperatures required in most previously reported systems. Substituting GVL with common organic solvents led to a sharp decrease in the 3A5AF yield (Fig. 5d), as these solvents often necessitate higher temperatures to activate the dehydration process. In contrast, GVL provides a unique solvation environment that lowers activation energy and enhances the reaction rate even under milder conditions. This environment is crucial for the efficient and selective conversion of NAG to 3A5AF, demonstrating GVL's superiority over the commonly used toxic solvents. In this study, we also explored the direct conversion of chitin to 3A5AF. Although the yield was relatively low of 16.0% under employed conditions, a two-step process involving chitin hydrolysis followed by NAG dehydration could offer a viable strategy for efficient 3A5AF production because the hydrolysis and dehydration require distinct optimal reaction conditions.

In addition to 3A5AF, other nitrogen-containing furanic compounds, such as chromogens, 3A5F and 3AF (Fig. 1), can be produced through the dehydration of chitin biomass. Several research groups have explored various non-catalytic and catalytic systems for the production of these compounds. The non-catalytic conversion of NAG under hydrothermal conditions without any additive yields chromogen I and chromogen III as the primary products, by eliminating one or two water molecules, respectively. Osada's group has utilized high-temperature water as an eco-friendly medium to dehydrate chitin monomers, dimers and polymers.<sup>79–82</sup> Under optimal conditions, NAG was dehydrated rapidly into chromogen I with a maximum yield of 37.0% at 180 °C, or into chromogen III with a peak yield of 34.5% at 240 °C under 250 bar.<sup>81</sup> Meanwhile, the



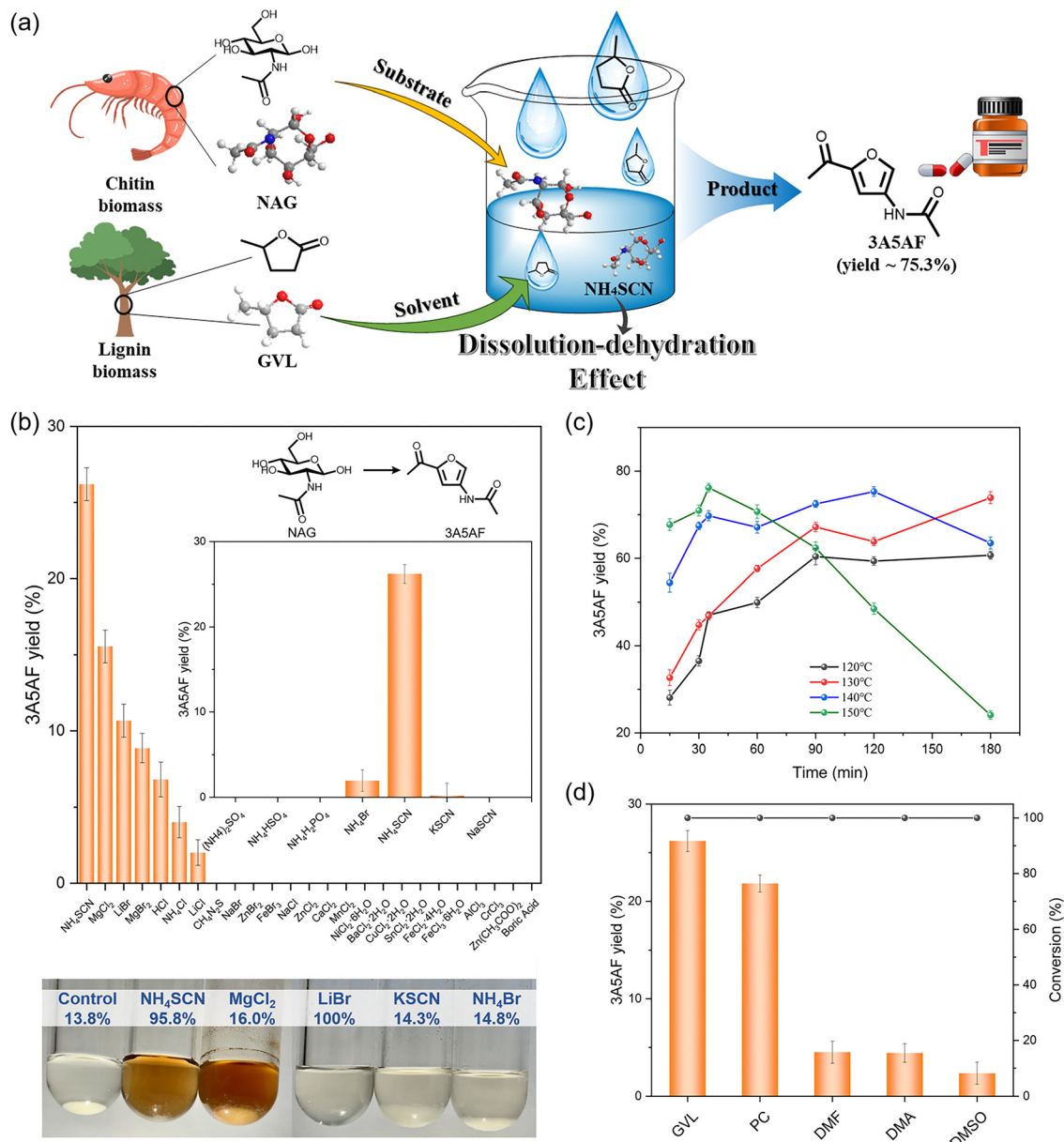


**Fig. 5** (a) The dissolution–dehydration effect on NAG conversion into 3A5AF in the presence of  $\text{NH}_4\text{SCN}$  and HCl catalysts in GVL. (b) Catalyst screening for 3A5AF production in GVL at 140 °C for 30 min and solubility tests of NAG in GVL at 140 °C for 2–3 min. (c) The effect of temperature and time on 3A5AF production in the presence of  $\text{NH}_4\text{SCN}$  and HCl catalysts in the GVL solvent. (d) The solvent effect on NAG conversion into 3A5AF in GVL at 140 °C for 30 min. Reproduced from ref. 78 with permission from Elsevier, copyright 2024.

selective synthesis of chromogen III was successfully achieved by Minnaard's group.<sup>83</sup> The use of phenylboronic acid and triflic acid as the promoters in the pyridine solvent led to the formation of Di-HAF in 73% yield with 99% enantiomeric excess. Building on these findings, 3A5F, a more reactive compound with an aldehyde group replacing the acetyl group, was produced in a two-step process for the dehydration and oxidative cleavage of NAG, with an overall yield of 92%.<sup>84</sup> Besides, the unsubstituted aminofuran 3AF was obtained in one step, with a maximal yield of 74%, *via* retro-aldol condensation–dehydration from NAG in the ternary  $\text{Ba}(\text{OH})_2$ – $\text{H}_3\text{BO}_3$ – $\text{NaCl}$  catalytic system.<sup>85</sup> These valuable compounds significantly

diversified the chemical scape of the chitin refinery. For example, 3A5F can undergo a variety of reactions such as reduction, reductive amination, aldol condensation, olefination, cyclopentenone and thiazolidine formation to access a series of fine chemicals.<sup>84</sup>

For the oxygen-containing furan-ring compound, 5-hydroxymethylfurfural (5-HMF), an analog of 3A5AF, has been widely regarded as “the sleeping giant” of sustainable chemistry.<sup>15</sup> Downstream products from 5-HMF can be obtained through various reactions, such as hydrogenation to form 2,5-dimethylfuran, oxidation to yield 2,5-furandicarboxylic acid or further conversion into levulinic acid.<sup>86,87</sup> Research on 5-HMF production has primarily

focused on its synthesis from carbohydrate-rich biomass, particularly *via* the dehydration of hexose sugars like glucose and fructose. In recent years, there has been growing interest in exploring chitin biomass as an alternative feedstock for 5-HMF production.<sup>88–90</sup> A variety of catalytic systems have been investigated, including mineral acids, metal salts and ILs.<sup>91–93</sup> Solvent systems such as polar aprotic solvents and biphasic mixtures have also been developed to improve both yield and selectivity.<sup>94–96</sup> Our group successfully converted various chitin biomass resources into 5-HMF in molten salt hydrates (MSHs).<sup>97</sup> The conversion of D-glucosamine in 65 wt% LiBr MSHs, with the addition of the boric acid catalyst, at 130 °C within 2 h, resulted in the highest 5-HMF yield of 49.6%. This reaction system was also applicable to glucose and NAG, which differs structurally from D-glucosamine only by the substitution group at position 2. It was observed that the amino group at position 2 is more conducive to 5-HMF production compared to the hydroxyl group, while the acetamido group significantly inhibits dehydration. To directly produce 5-HMF from the polymers, the Box-Behnken design method was employed to optimize reaction conditions while minimizing the number of experiments. As a result, 5-HMF was obtained from chitosan and chitin with yields of 21.6% and 15.3%, respectively, by adding a catalytic amount of HCl. This study provided valuable insights into chitin refinery through the use of experiment-assisted tools.

## Amino/amide sugars

Amino/amide sugars (NAG, D-glucosamine, oligomers and their derivatives) are a group of valuable products that could be obtained through chitin depolymerization. Chitin depolymerization could involve the hydrolysis of the glycosidic bond and the acetamido group. The complete hydrolysis of the glycosidic bond yields a NAG monomer, valuable for applications in the pharmaceutical and nutraceutical industries. Concurrently, the acetamido group can also undergo hydrolysis to form D-glucosamine, a deacetylated monomer known for its bioactivity and versatility in various applications. In addition to primary hydrolysis reactions, the side chains of chitin, rich in reactive hydroxyl groups, can undergo various chemical transformations, leading to a wide array of chitin monomeric and oligomeric sugar derivatives, thereby expanding the scope of chitin's applications. These derivatives, as well as amino/amide sugars, can be converted into various downstream products, including amino acids, pharmaceutical compounds, glycosidic conjugates, *etc.*,<sup>98,99</sup> through a variety of chemical reactions, thereby expanding the scope of chitin's applications.

Traditional methods for producing chitin-derived sugars rely on concentrated acid or enzymatic processes, which are costly, environmentally concerning, or exhibit low product selectivity.<sup>100–102</sup> Consequently, the development of greener and more efficient alternative approaches is urgently needed. Recent explorations into new solvent systems have revealed that novel solvents can interact strongly with the functional groups on chitin, thereby breaking down its highly ordered structure and enhancing the depolymerization process. One feasible approach was the liquefaction of chitin in ethylene glycol (EG),<sup>103</sup> where up to 75% of chitin was liquefied

using 8 wt% sulfuric acid at 165 °C within 90 min. The major products were identified as hydroxyethyl-2-amino-2-deoxyhexopyranoside (HADP) and hydroxyethyl-2-acetamido-2-deoxyhexopyranoside (HAADP), with a cumulative yield of 30%. EG played a dual role in the liquefaction process: it disrupted chitin's crystalline domains to improve solubility, and then it attacked the glycosidic bonds to afford HAADP, which subsequently underwent deacetylation to produce HADP owing to nucleophilic attack from EG (Fig. 6). Similarly, Yan' group reported that formic acid (FA) facilitated the liquefaction of ball-milled chitin without any additional catalyst.<sup>104</sup> FA functioned as a solvent, catalyst and formylation reagent in this reaction, resulting in a series of monomeric products, including formic acid-derived NAG, dehydration products and 5-(formyloxy-methyl)furfural (FMF), with an overall yield of up to 60% at 100 °C for 12 h. As the reaction time extended, the product stream gradually converged towards a single compound, FMF, with a yield of 35%. The use of these organic solvents could lower the acid dosage as compared to the traditional methods (*e.g.* using 35% mineral acids) primarily because the interactions/derivations of the solvent molecules with the chitin polymers impair the hydrogen bond networks and/or the crystallinity.

Aside from pure organic solvent systems, water/organic co-solvent systems not only accelerated the hydrolysis of glycosidic bonds but also increased the deacetylation rate with diluted acid as the catalyst, yielding the deacetylated monomer and oligomer. Yan's group pioneered the study of these systems, demonstrating their effectiveness in the production of amino sugars. They designed a series of combinations of water and different polar aprotic solvents, achieving an 80% yield of D-glucosamine from ball-milled chitin at 175 °C within 1 h.<sup>105</sup> The optimized co-solvent, determined to be a 4:1 ratio of diethylene glycol diethyl ether (DGDE)/water, significantly reduced the concentration of the sulfuric acid catalyst to merely 0.1 M. Based on the solvent screening and solvent property analyses, hydrogen bond basicity and hydrogen-bonding interaction were identified as the key parameters to promote the production of D-glucosamine in the co-solvent system. The optimal DGDE/water showed lower hydrogen bond basicity and an appropriate level of hydrogen-bonding interactions, which respectively increased the apparent acidity of the system and promoted chitin solubility. In another study, Yan's group reported a co-solvent system containing 5 wt% sulfuric acid solution and 10 wt% formaldehyde in water,<sup>106</sup> which efficiently converted chitin polymers into *N,N*-dimethyl chitosan oligosaccharides (DMCOS) through a tandem depolymerization-deacetylation-*N*-methylation process. In this process, chitin first underwent depolymerization and deacetylation to generate chitosan oligosaccharides (COS) under the catalysis of sulfuric acid. The COS then reacted with formaldehyde *via* an adjacent hydroxyl group-assisted mechanism to produce DMCOS, achieving an optimal yield of 77%. This product exhibited a high degree of deacetylation and methylation, along with notably reduced average MW. DMCOS demonstrated superior antifungal activity compared to chitosan and other reported chitosan oligosaccharide derivatives, paving the way for the development of novel antifungal agents derived from chitin.



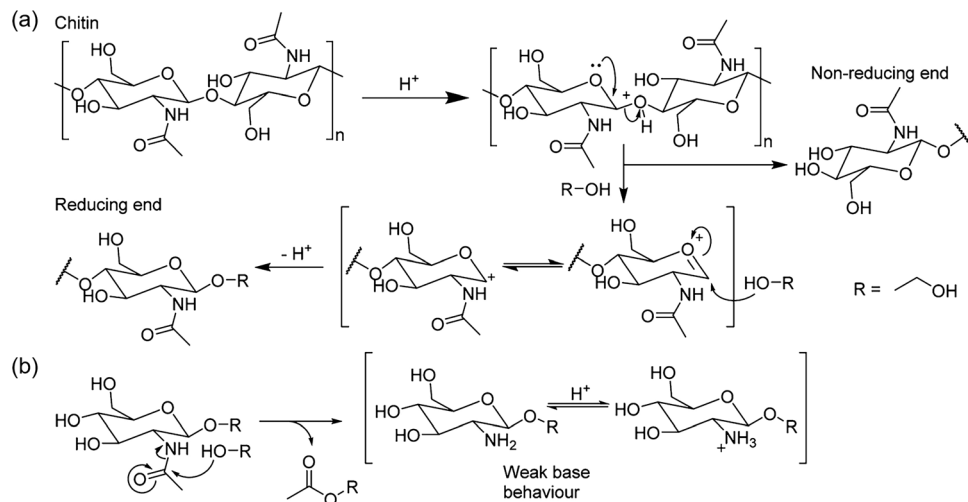


Fig. 6 Proposed reaction pathways for chitin liquefaction in EG: initial solvolysis (a) and sequential deacetylation (b). Reproduced from ref. 103 with permission from American Chemical Society, copyright 2014.

The MSH solvent has been developed for highly selective conversion of chitin into the NAG monomer. The MSHs that are formed from inorganic salts and water with a water-to-salt ratio approximating the saturated coordination number of the dominant hydrated cations have minimized the number of water molecules in the solvation shell.<sup>107</sup> Usually, there is only one hydration layer around the cation in MSHs with negligible free water outside the layer compared to dilute or concentrated solutions (Fig. 7a). This would cause obvious polarization of the water molecules and lead to significantly increased apparent acidity, which would notably decrease the acid dosage that is needed for the cleavage of the glycosidic bonds. With the reduced acid dosage, the glycosidic bonds are probably prone to be cleaved while the acetamide side group remained unbroken, which then exclusively enhanced the product selectivity towards NAG. Yan's group pioneered the use of MSHs for selective chitin hydrolysis, reporting LiBr MSHs as the most effective type for this process.<sup>108,109</sup> The highest yield of NAG beyond 70% was realized using only 0.04 M HCl at 120 °C for 0.5 h in the 60 wt% LiBr MSH solvent. The main reasons for the effectiveness of LiBr for chitin hydrolysis were ascribed to the much-boosted apparent acidity (superacidic properties) and the enhanced chitin swelling/dissolving ability because the Li cation strongly coordinated with the hydroxyl groups to disrupt the hydrogen bond networks. The Li cation boasted a small radius and the Br anion possessed relatively large radius, and therefore, the ions were easy to dissociate and had a good ability to interact with chitin polymers. Later on, the same group attempted the use of acidic zeolites as the solid acid catalyst to replace HCl for the hydrolysis; nevertheless, the protons on the zeolites exchanged with the Li cation in the solvent and eventually the hydrolysis was homogeneously catalyzed by the leached protons.

Following these works, our group has explored the possibilities of using less expensive, greener and more abundant salt species as the MSH solvent for selective chitin hydrolysis.<sup>110</sup> First, a group

of inexpensive salts (NaCl,  $MgCl_2$ ,  $CaCl_2$ , etc.) have been examined and only  $CaCl_2$  showed certain activity despite the NAG yield being relatively low (~5%). To improve the yield, a mild, low-cost and easy-to-scale aging method has been employed to impair the robustness of chitin prior to hydrolysis. The chitin powder was first aged in the presence of a small amount of sulfuric acid (at a 1 : 8 ratio to chitin) at near room temperature for 48 h, followed by hydrolysis in a 50 wt%  $CaCl_2$  MSH solution at 120 °C for 1 h. The aging-hydrolysis integrated method achieved an impressive 51.0% NAG yield in  $CaCl_2$  MSH, which was ten-fold as that from unaged chitin. Besides, the NAG yield increased to 66.8% with the addition of  $ZnBr_2$  as a co-salt. The aging process and  $CaCl_2$  MSHs synergistically promoted efficient chitin hydrolysis. The mild aging process substantially reduced the MW of chitin, possibly decreasing the energy barrier and facilitating subsequent hydrolysis; meanwhile, the  $CaCl_2$  MSHs promoted chitin swelling and dissolution. NMR (Fig. 7b) analyses confirmed the intimate interaction between chitin and  $CaCl_2$ . The significant shift of specific peaks assigned to the acetamido group on NAG has been observed in the NAG with  $CaCl_2$   $D_2O$  samples from the  $^{13}C$  NMR spectra. Specifically, as proposed in Fig. 7c,  $Ca^{2+}$  cations coordinated with the carbonyl oxygen and amido nitrogen atoms, while  $Cl^-$  anions formed hydrogen bonds with the hydroxyl groups. These interactions modified the electrostatic properties of the chitin chains, thereby enhancing the efficiency of the hydrolysis process.

Besides utilizing the solvent effect, ball milling or mechanochemical conversion, a process combined with both mechanical and chemical forces capable of inducing chemical transformations, has emerged as a promising technique for chitin depolymerization. This process disrupts chitin's high crystallinity and robust structure, facilitating its depolymerization into products with varying degrees of polymerization (DP).<sup>111</sup> In the acid-catalyzed ball milling approach, the *N*-acetyl group on chitin is typically well-preserved. Fukuoka's group demonstrated that ball

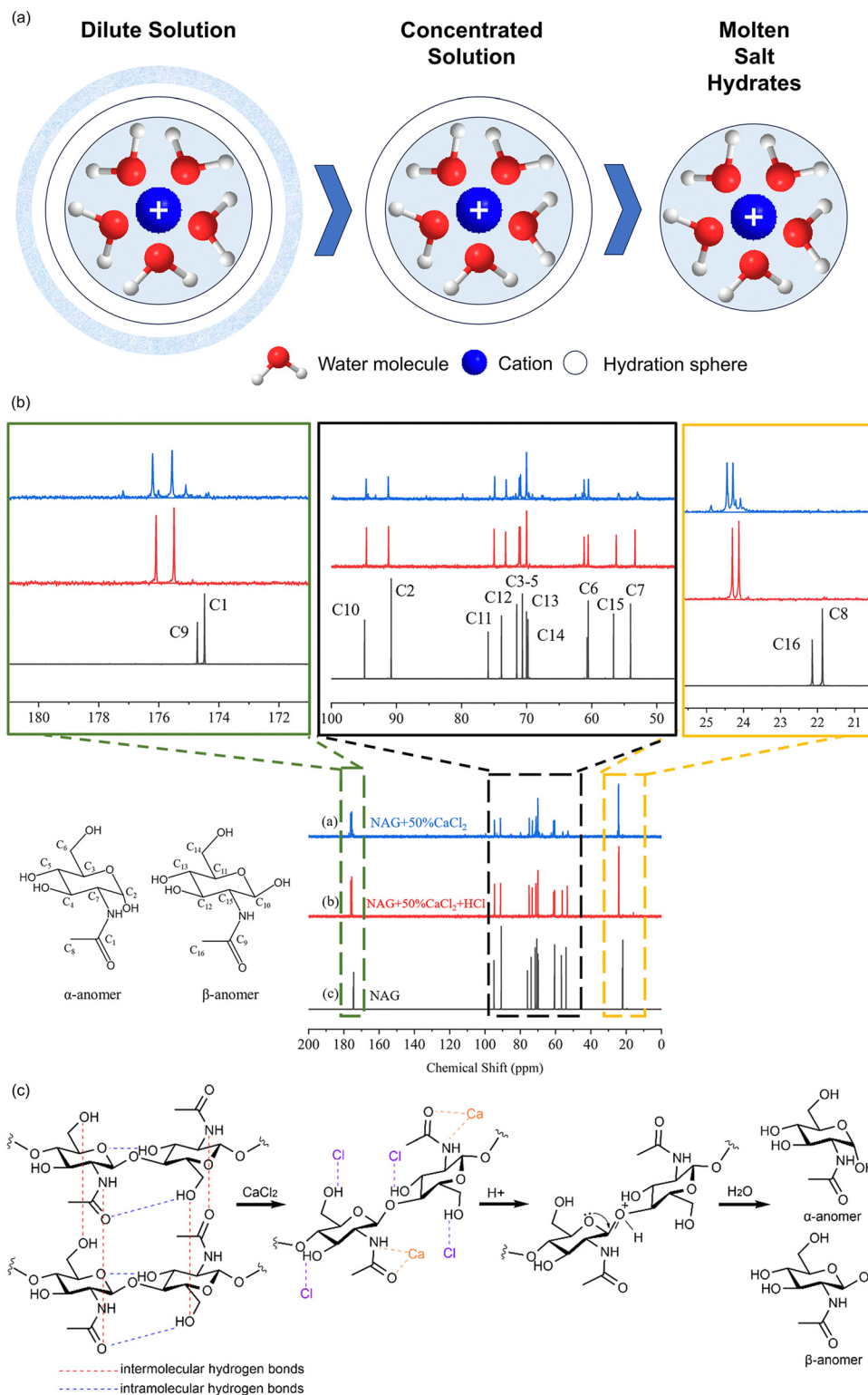


**Fig. 7** (a) Graphical depiction of salt solutions with varying salt concentrations. The interaction between chitin and  $\text{Ca}^{2+}$  cations and  $\text{Cl}^-$  anions. (b)  $^{13}\text{C}$  NMR spectra of NAG and  $\text{CaCl}_2$ . (c) The proposed interaction mode between chitin and  $\text{Ca}^{2+}$  cations and  $\text{Cl}^-$  anions. Reproduced from ref. 110 with permission from The Royal Society of Chemistry, copyright 2023.

milling acid-impregnated chitin powders at 500 rpm for 6 h under solid-state conditions, using physically adsorbed water in chitin as a reagent, resulted in the formation of soluble short-

chain oligomers, which could be hydrolyzed to NAG (53% yield) or methanolized to 1-O-methyl-N-acetylglucosamine (70% yield).<sup>112</sup> This outcome occurs because the mechanical forces

applied to the polymer chain selectively cleave glycosidic bonds in preference to the acetamido group within an acidic environment.<sup>113</sup> Additionally, Fukuoka's group showed that employing a carbon-based catalyst with weak acid sites during the milling process allowed for high selectivity (up to 94%) towards chitin oligosaccharides with a low degree of polymerization (DP of 1 to 6),<sup>114</sup> which pioneered the heterogeneous catalysis for efficient chitin depolymerization. Under basic conditions, not only the glycosidic bonds but also the acetamido bonds could be cleaved to afford low-molecular-weight chitosan (LMWC) products. Our study conducted the ball milling of chitin together with different types of bases such as NaOH in a solid state.<sup>115</sup> The Fourier-transform infrared spectroscopy (FTIR) analysis (Fig. 8a) of the NaOH-700-8 sample (chitin ball milled in the presence of an equivalent mass of NaOH at a speed of 700 rpm for 8 cycles was denoted as NaOH-700-8) closely

matched that of commercially available chitosan (chitosan-C), with all characteristic peaks aligning perfectly, which indicated that deacetylation effectively occurred during the base-catalyzed mechanochemical process. The gel permeation chromatography (GPC) results (Fig. 8b) showed that the addition of a basic catalyst reduced the MW of the NaOH-700-8 sample to merely 8.5 kDa, down from the initial 362.4 kDa, much lower than both chitosan-C (239.1 kDa) and chitosan-H (homemade chitosan from chitin) (149.3 kDa). These results highlight that while mechanical milling causes some depolymerization of chitin, the presence of a base greatly enhances this effect. As a result, simultaneous deacetylation and depolymerization of chitin occurred in a single step, yielding LMWC with a narrow MW distribution and a polydispersity index of only 1.1. The required base amount was reduced to approximately one-tenth of typical usage, significantly reducing environmental impact. In this process, varying ball milling parameters such as speed, time and the number of balls can adjust the degree of deacetylation and MW, offering a versatile method for tailoring LMWC properties with DP ranging from 7 to 80 monomer units and DA ranging from 39.1% to 83.3%. The DP of the products was higher than those using acid catalysts because the cleavage of glycosidic bonds was more favorably catalyzed by an acid. In addition to our work, Moores' group has adopted a mixing milling machine, considered a milder mechanochemical method compared to the planetary ball milling used in most previous studies. They further enhanced the process by combining aging with a base such as NaOH.<sup>116</sup> By controlling the aging and milling conditions, the glycosidic bonds could be well reserved while the acetyl side chain could be efficiently cleaved to obtain high-molecular-weight chitosan (HMWC) products. As a result, with different ball milling protocols, both LMWC and HMWC products could be directly obtained from chitin in a green, nearly-quantitative and solvent-free manner, and these products would have distinct applications in a broad range of areas such as material synthesis, pharmaceuticals, biomedical, agricultures, foods, *etc.*

## Organic acids

Organic acids represent a group of value-added compounds with significant applications for the chemical industries. For instance, formic acid (FA) serves as a solvent in organic synthesis,<sup>117</sup> while acetic acid (AA) is a key building block for producing solvents, esters, and polymers such as acetate fibers.<sup>118</sup> The production of organic acids, including AA, from renewable biomass resources has been extensively investigated.

Early research by Koichi *et al.* explored the hydrothermal oxidation of glucose using hydrogen peroxide to produce AA.<sup>119</sup> Although hydrogen peroxide enhanced the oxidation process, the yields remained low. To improve this, Jin's group developed a two-step strategy.<sup>120</sup> In the first step, cellulose was converted into intermediates, which were then oxidized to AA in the second step. The process could be either acidic or alkaline, depending on the additives used. For example, under acidic

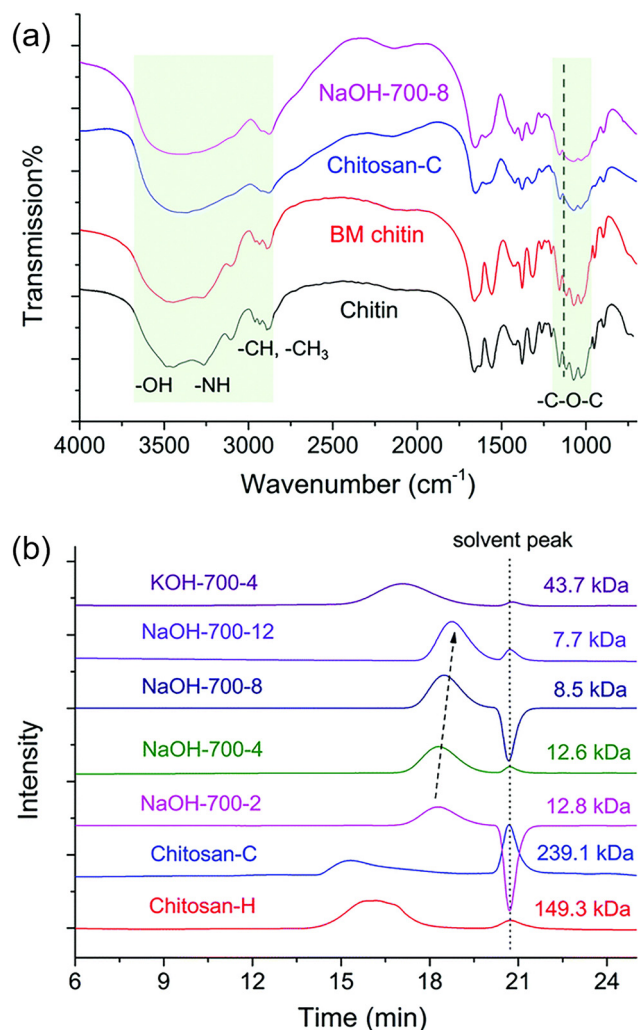


**Fig. 8** (a) FTIR analysis of chitin, BM chitin, chitosan-C and NaOH-700-8. (b) GPC spectra of chitosan-C, chitosan-H and the products obtained with different milling times and bases (The chitin sample ball milled in the presence of a base was denoted as the base type-speed-cycle time). Reproduced from ref. 115 with permission from The Royal Society of Chemistry, copyright 2017.



conditions, 5-HMF was first produced from monosaccharides, which were then converted to levulinic acid and further oxidized to AA. This method achieved an AA yield of up to 26% from glucose.<sup>120</sup> In contrast, an alkaline process using calcium hydroxide resulted in an AA yield of 27% from glucose.<sup>121</sup>

Chitin, with its acetyl amino side chain, offers inherent advantages for AA production compared to other biomass resources. Theoretically, by hydrolyzing the acetamide side chain alone, an AA yield of up to 25% could be achieved. Further decomposition and oxidation of the chitin main chain could potentially increase the yield even further. Our group has undertaken several works to obtain AA and other organic acids from chitin biomass. We have fabricated the non-noble metal CuO as the catalyst to promote direct chitin conversion under hydrothermal conditions.<sup>122</sup> An AA yield of up to 38.1% could be achieved under 5 bar oxygen gas at 300 °C in 2 M NaOH solutions from chitin polymers, and the yield could increase to 47.9% with raw shrimp shell powders as the substrate because proteins in the shell also contributed to the formation of AA. In this process, the CuO acted as an efficient catalyst to promote the oxidation. Based on the characterization, the lattice oxygen in CuO was the real oxidative species, and CuO could be transformed to Cu<sub>2</sub>O during the reaction, which will be

regenerated to CuO by the oxygen gas to complete a catalytic cycle. Several interconnected pathways have been proposed to explain the conversion of chitin into final products (Fig. 9), including AA and other organic acids. The process began with the deacetylation and deamination of chitin under alkaline conditions, leading to the formation of D-glucosamine. AA was primarily released during this stage through the hydrolysis of the acetyl side chains. The deaminated D-glucosamine was subsequently converted into glucose, which underwent fragmentation *via* retro-aldol reactions, producing smaller organic compounds such as LA and glyoxylic acid. Upon the introduction of an oxidant, some of these intermediates were further oxidized to acetic acid. This demonstrated that acetic acid is not only derived from the hydrolysis of acetyl side chains but also from the oxidative degradation of sugar intermediates, positioning chitin as an advantageous resource to produce AA.

To mitigate the environmental impact caused by concentrated alkaline solutions, we further designed a base-free, vanadium-catalyzed oxidation system that converted chitin biomass into AA under relatively milder conditions.<sup>123</sup> Under a low oxygen pressure (5 bar) and in the absence of a base, the highest yield of AA reached 33.4% from the chitin monomer NAG and 30.0% from the ball milled chitin polymer at 220 °C

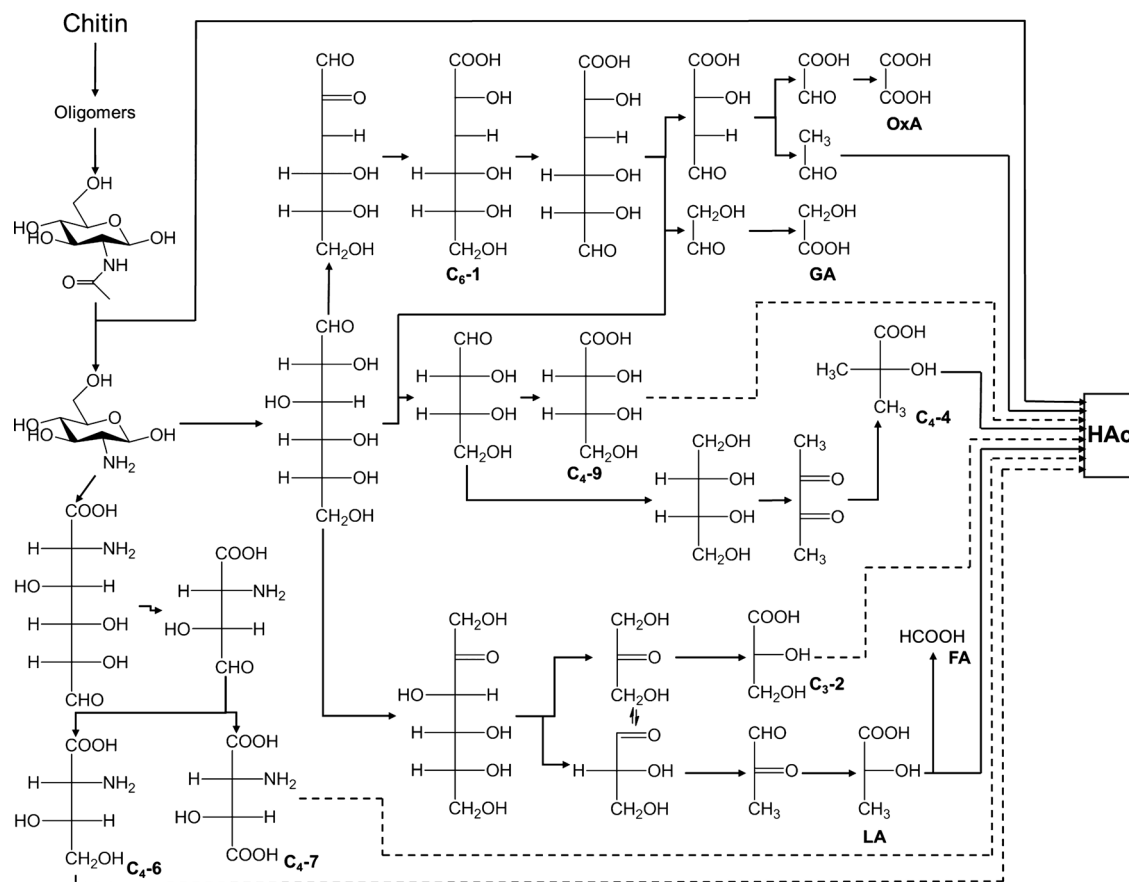


Fig. 9 Proposed reaction networks of chitin conversion into AA and other organic acids under the catalysis of CuO in the NaOH solution (solid line: the plausible pathway with experimental evidence and dashed line: the speculated pathway.) Reproduced from ref. 122 with permission from American Chemical Society, copyright 2016.

under the catalysis of the  $V_2O_5$  catalyst in water. Based on various characterization methods and control experiments, we proposed the following possible reaction pathways for generating AA from chitin in this catalytic system (Fig. 10). The chitin polymer was first hydrolyzed into oligomers and monomeric sugars, followed by the cleavage of the acetyl amino side chain. The resulting short-chain intermediates were then oxidized to form AA. Simultaneously, the glucolactone intermediate may undergo cleavage at different positions, producing various small organic acids. These compounds were unstable under catalytic oxidation conditions, leading to the gradual accumulation of a few stable, simple organic acids, such as AA, as the reaction progressed, which accounted for the excess production of AA.

To mitigate the energy requirement and carbon footprints, it would be more desirable if transformations proceed under near room temperature and low pressure, which better meets the demand for green synthesis and sustainable development. Our group has attempted the possibilities of converting chitin monomers into key organic acids under much milder temperatures than previous works. The conversion of the chitin monomer NAG could be activated under basic conditions under ambient temperature and pressure. By introducing different oxidants, the oxidation reaction could more efficiently occur to produce specific organic acids. Based on these observations, we devised a selectivity-switchable way to transform NAG into different valuable organic acid products, such as FA and AA,

at near room temperature ( $35\text{ }^\circ\text{C}$ ) in a dilute NaOH solution (0.6 M).<sup>124</sup> Under an oxygen atmosphere (5 bar oxygen gas), the main products were AA and glyceric acid (GlyA), which could be obtained with a combined yield of 41.2%. By employing  $H_2O_2$  as the oxidant, FA production was dominant. The FA yield correspondingly increased as the concentration of hydrogen peroxide increased and reached a peak value of 57.1% with 92.2% NAG conversion in 1.6 M  $H_2O_2$  solution. (Fig. 11a). This selectivity change was attributed to the differing stability of intermediate compounds formed during the oxidation process, where the oxidant finely tuned the primary pathways to determine the specific product distributions. The reaction pathway started with the base-catalyzed deacetylation and deamination of NAG, producing D-glucosamine and other intermediates. The acetyl side chain is hydrolyzed, contributing to the AA formation. Additionally, epimerization of NAG into N-acetyl-D-mannosamine occurred, followed by retro-aldol condensation, which cleaved the sugar backbone and generated smaller molecules such as GlyA and glycolic acid. To summarize, the use of different oxidants determined the dominant reaction products (Fig. 11b): in the presence of oxygen, the oxidative cleavage of aldehyde intermediates enhanced the formation of AA and GlyA, with an overall selectivity of 43.6%. While using  $H_2O_2$  led to a shift towards formic acid, with FA selectivity reaching 62.4%, as the oxidative cleavage of the C–C bond was promoted by radical-induced cleavage mechanisms.

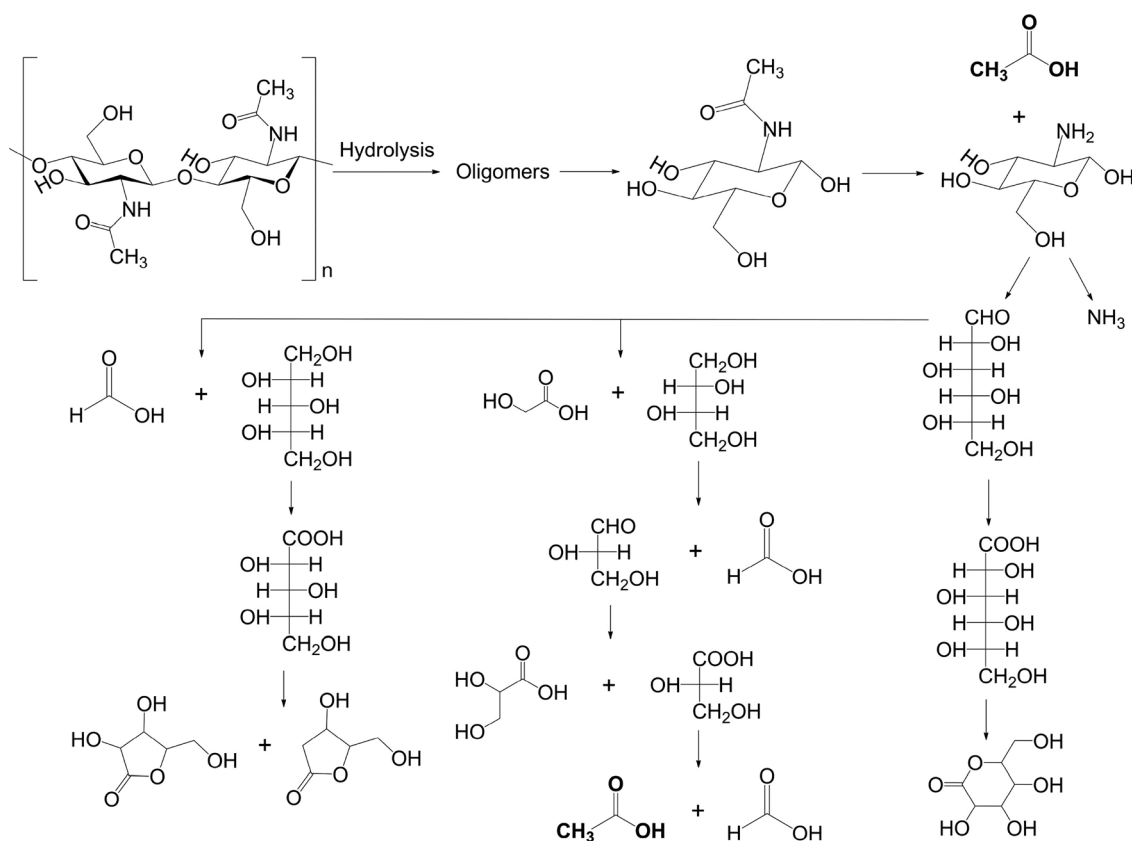


Fig. 10 Proposed reaction pathway of AA formation from chitin under the catalysis of  $V_2O_5$  in water. Reproduced from ref. 123 with permission from American Chemical Society, copyright 2020.

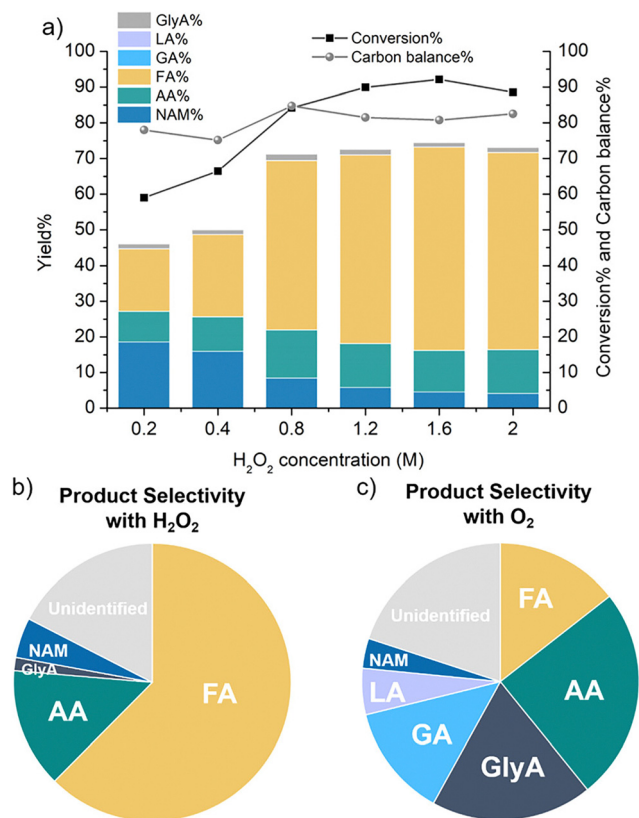


Fig. 11 (a) NAG conversion with the addition of H<sub>2</sub>O<sub>2</sub>. (b) Product selectivity in 2 M H<sub>2</sub>O<sub>2</sub> aqueous solution. (c) Product selectivity under 5 bar O<sub>2</sub> gas. Reproduced from ref. 124 with permission from American Chemical Society, copyright 2021.

## Amino/amide acids

Amino acids/amide acids are high-value key chemicals for the synthesis of proteins, functional materials, bioactive pharmaceuticals and so on. For example, D-glucosaminic acid plays a crucial role in the biosynthesis of glycoproteins and glycolipids by serving as a precursor in the formation of sugar moieties that are essential for these biomolecules.<sup>125</sup> Relevant amino/amide acid sugars could be easily obtained from chitin biomass *via* the hydrolysis–oxidation strategy (Fig. 12). In chitin hydrolysis, the sugar monomers such as NAG and D-glucosamine could be readily formed, in which the aldehyde group at the end boasts high reactivity and is susceptible to be selectively oxidized by specific catalysts. In this way, the amino acid products N-acetyl-D-glucosaminic acid and D-glucosaminic acid could be produced, respectively. Furthermore, if retro-aldol condensation occurs to cleave the C–C bonds of the sugar monomers, followed by oxidation of the aldehyde group, then the shorter chain amino acid product N-acetyl glycine (AcGly) could be accessible from chitin. So far, these were the major amino acid products that have been reported to be catalytically obtained from chitin biomass.

The one-step conversion of chitin or chitosan into the corresponding amino acids was rather difficult and has not been realized so far, probably because the catalytic systems and

the reaction conditions required for hydrolysis and oxidation are normally quite different. Yan's group has put forward a two-step tandem approach to directly convert chitosan into D-glucosaminic acid with an overall yield of 36%.<sup>126</sup> Amberlyst-15 was employed as the solid acid catalyst to promote chitosan hydrolysis while Au/MgO was utilized for the subsequent oxidation under oxygen gas to produce D-glucosaminic acid. This oxidation step required the precise control of reaction conditions to achieve optimal yields. However, a detoxification process by using activated carbon was necessary after the hydrolysis step, which could effectively remove the inhibitory by-products (humin-like polymers) that would poison the Au catalyst in the oxidation step from the hydrolysate.

The direct oxidation of chitin monomer sugars into the corresponding amino acid sugars with high yields under mild conditions has been well studied by Ebitani's group.<sup>127</sup> The synthesis of D-glucosaminic acid from D-glucosamine-HCl was catalyzed by Au nanoparticles (NPs) supported on basic MgO, conducted at 40 °C for 3 h with an O<sub>2</sub> flow of 50 mL min<sup>−1</sup>, achieving a maximum yield of 93%. Additionally, using Au NPs supported on another basic material, HT, N-acetyl-D-glucosaminic acid was produced from NAG at 25 °C for 5 h with an O<sub>2</sub> flow of 30 mL min<sup>−1</sup>, with a yield of 95%. Recently, our group synthesized Au NPs on ZnO supports to oxidize the D-glucosamine into D-glucosaminic acid in atmospheric air for the first time.<sup>128</sup> Among the metal oxide supports tested, as shown in Fig. 13a, ZnO displayed the best performance in the formation of D-glucosaminic acid, compared to others such as CeO<sub>2</sub>, ZrO<sub>2</sub>, and TiO<sub>2</sub>, because the interaction between Au NPs and the ZnO support prevented the NP aggregation, maintaining the small particle sizes which are critical for high catalytic activity. Among the synthetic methods, the Au/ZnO catalyst prepared by the deposition–precipitation (DP) method outperformed the catalyst prepared by the deposition–reduction method, achieving an 85% yield of D-glucosaminic acid at 35 °C in pure water without any base addition (Fig. 13b). This high performance was linked to the lower apparent activation energy required for D-glucosaminic acid production with the DP-prepared catalyst. Transmission electron microscopy (TEM) and X-ray photoelectron spectroscopy (XPS) analyses (Fig. 13c and d) revealed that the DP method produced smaller, more uniformly dispersed Au NPs on ZnO, along with a higher proportion of metallic Au (Au<sub>0</sub>) and increased oxygen vacancies (O<sub>v</sub>), both of which were associated with the catalyst's enhanced activity.

In comparison to the C<sub>6</sub> amino acid, the production of shorter-chain amino acid from NAG is more challenging as the optimal reaction conditions for C–C bond cleavage and subsequent oxidation differ from each other. Fukuoka's group reported the conversion of NAG into AcGly in the presence of the Ru/C catalyst and NaHCO<sub>3</sub> additive *via* the tandem retro-aldol condensation–hydrogenation–oxidation reaction.<sup>129</sup> Firstly, the reaction was conducted at 120 °C for 1 h. During this stage, the C–C bond cleavage of the sugar chain occurred to generate the shorter-chain intermediate, which was hydrogenated into NMEA under a gradient-increased H<sub>2</sub> pressure from 1 to 40 bar. Next, after the atmosphere was adjusted



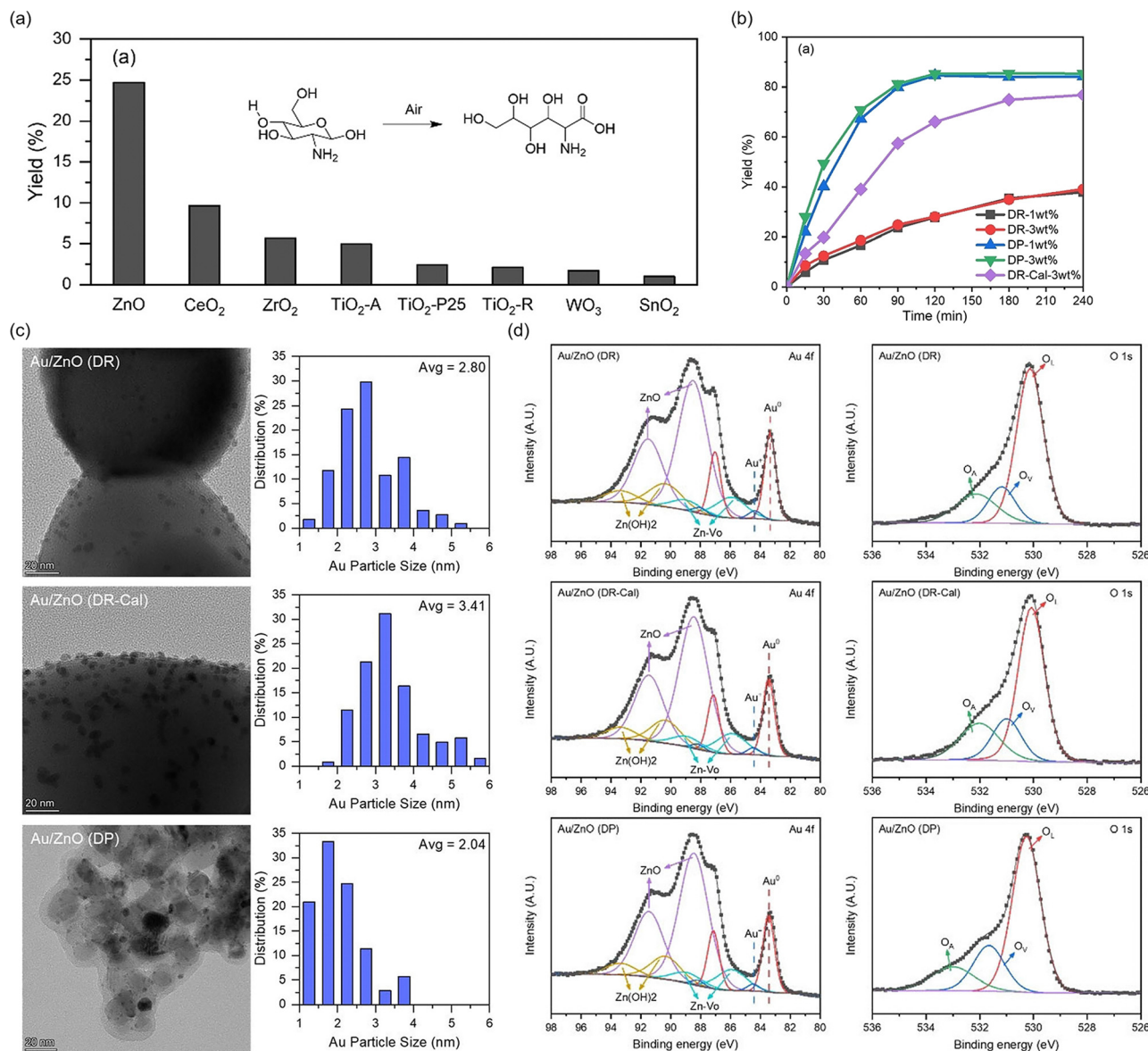


Fig. 12 The amino/amide acid sugar production from chitin biomass via the hydrolysis-oxidation strategy.

to 10 bar O<sub>2</sub>, the reaction continued to proceed at 120 °C for 1 h, where NMEA was oxidized into AcGly with the highest yield of 21%. However, the catalytic system was not considerably selective as the overall yield of major by-products was over 50%. Following this, Dai *et al.* developed a homogenous strategy for the aerobic oxidation of NMEA into AcGly.<sup>130</sup> With the combinational use of Fe(NO<sub>3</sub>)<sub>3</sub>, TEMPO and KCl in the 1,2-dichloroethane solvent, the peak 62% yield of AcGly could be achieved at 35 °C with a reaction time of 16 h under 20 bar O<sub>2</sub> gas. Initially, Fe(NO<sub>3</sub>)<sub>3</sub>·9H<sub>2</sub>O and TEMPO coupled to form an active complex that triggered the oxidation of NMEA, which subsequently decomposed into an intermediate, acetylacetaldehyde amine. During this process, the oxidized form of TEMPO (TEMPOH) was recycled back to its active form by Fe(NO<sub>3</sub>)<sub>3</sub>·9H<sub>2</sub>O. The NO<sub>3</sub><sup>-</sup> ion from the iron salt engaged in a NO<sub>x</sub> cycle, where it participated in the re-oxidation of Fe(II) to

Fe(III), with O<sub>2</sub> acting as the terminal oxidant. The water molecules then assisted in the final step of converting the intermediate into AcGly, closing the catalytic cycle, thus sustaining the catalytic cycle for the oxidation process.

## Conclusions and perspectives

The unique structure of chitin positions it as a versatile and valuable feedstock for generating a wide range of key platform chemicals through various chemical transformations. The first step in unlocking the potential of chitin is the fractionation of shrimp shells—the largest source of chitin. Drawing inspiration from the principle of tenderizing meat proteins in a pressure cooker and the formation of stalactites, we developed an environmentally friendly process, named HOW-CA, which

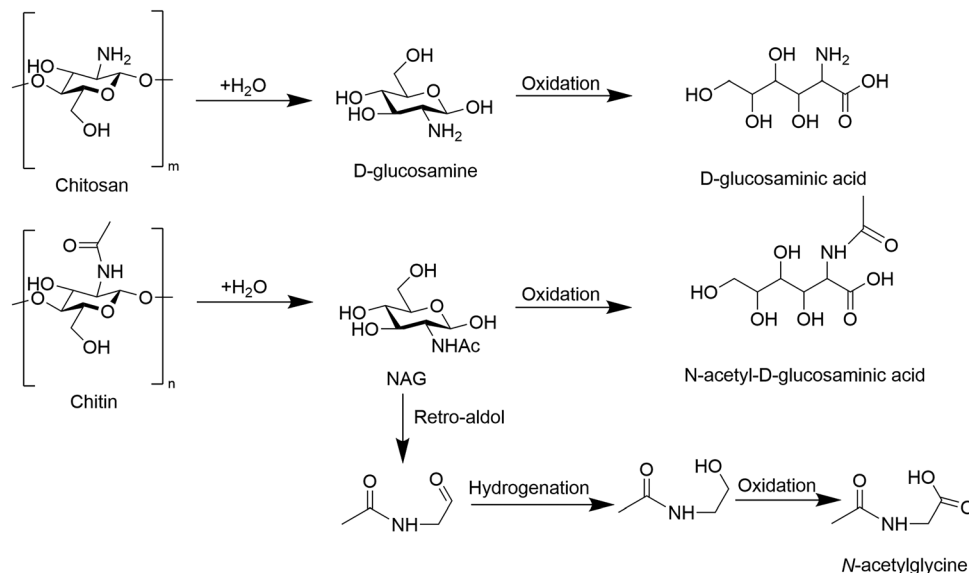


**Fig. 13** (a) The yield of D-glucosaminic acid with Au NPs on different supports as the catalysts. The influence of different preparation methods on (b) the D-glucosaminic acid yield curve. (c) The TEM images and corresponding size distributions and (d) Au 4f and O 1s XPS spectra of different catalysts. Reproduced from ref. 127 with permission from Wiley-VCH GmbH, copyright 2022.

uses hot water as the deproteinization reagent and carbonic acid as the demineralization reagent, successfully extracting chitin from shrimp shells with a purity exceeding 90%. The HOW-CA process not only matches the efficiency of existing extraction techniques but also offers a green and economical alternative, significantly enhancing the feasibility and competitiveness of chitin refinery. Additionally, chitin is also present in insect exoskeletons and fungal cell walls. As the chitin industry expands, more efficient extraction methods from these sources are expected to emerge.

Regarding furanic compounds, the current studies efficiently converted chitin biomass into specific dehydration products, such as 3A5AF, 3A5F, and 3AF, with high yields; however, most of the processes use homogeneous catalysts, which pose challenges related to product separation and catalyst reusability, making large-scale production of 3A5AF difficult at an industrial level. Future efforts should focus on developing solid catalysts with both Brønsted and Lewis acid sites, along with practical separation and purification methods. From a green chemistry perspective, the bio-based solvent GVL has been identified as providing a unique solvation environment that facilitates high-yield production of 3A5AF under milder conditions. Additionally, preliminary experiments suggest the potential of another green solvent, propylene carbonate, which warrants further investigation. The development of closed-loop solvent recovery systems, coupled with advancements in scalable, low-carbon methodologies, will be crucial for industrial applications.

In amino/amide sugar production, the recalcitrant structure of chitin presents major challenges for its selective hydrolysis into NAG or D-glucosamine. Novel solvents can interact with chitin's functional groups, altering its hydrogen-bonding structure to promote swelling and/or dissolution. These solvents can

also increase the system's apparent acidity, enabling hydrolysis with much lower acid loading compared to traditional methods. In organic solvents, chitin can be liquefied into monomeric derivatives under milder conditions, though selectivity issues arise due to the presence of multiple reactive groups on the side chain. It is beneficial to develop water/organic co-solvents with low hydrogen bond basicity and moderate hydrogen-bonding interactions to enhance D-glucosamine selectivity under acid-catalyzed conditions. Alternatively, MSHs have also been effective in selectively hydrolyzing chitin into NAG, but further research is needed to understand the synergistic effects between different MSH species and to optimize the separation of NAG from MSHs. Beyond liquid-phase strategies, ball milling can disrupt the chitin's crystalline structure, improving its depolymerization. Future research should focus on developing solid catalysts to improve selectivity and reduce the need for additives, as well as optimizing energy-efficient milling techniques to lower energy consumption and minimize the environmental impact of chitin depolymerization.

For organic acid production, FA, AA and several small-molecule acids have been demonstrated accessible from chitin biomass, and chitin is a superior starting material to lignocellulosic biomass especially for AA production. However, the complex structure of chitin currently results in low selectivity for specific acids within existing catalytic reaction systems. To improve yields, it is essential to develop new catalysts that enhance the decomposition and oxidation of the chitin chain, allowing for product convergence to a single compound. Besides, future efforts should also focus on innovative strategies to leverage the chitin's unique structure for upgrading it into value-added acids.

For amino/amide acid production, Au NPs exhibit high selectivity and activity in NAG oxidation. Future research

directions include exploring non-noble metals capable of selectively catalyzing the oxidation of monomers into amino acids as a cost-effective alternative to Au NPs. While oxidizing their monomers is relatively straightforward, the direct oxidation of chitin or chitosan into amino acids remains a significant challenge. Further exploration into multifunctional catalytic systems that combine hydrolysis and oxidation in one step could offer new pathways for directly producing high-value amino acids from chitin biomass.

To date, the reaction mechanisms involved in chitin transformations have not been fully clarified, limiting the development of certain transformation routes. The integration of computational modeling and experimental techniques to better understand these complex mechanisms could provide valuable insights and guide the design of more efficient and selective processes.

We anticipate that these advancements in the catalytic conversion of chitin biomass will pave the way for the practical utilization of chitin, thereby creating a multitude of opportunities to produce key platform chemicals through the chitin refinery.

## Author contributions

XJ: writing – original draft and visualization; YL: writing – original draft; XC: writing – review and editing.

## Data availability

This feature article does not involve the generation of new datasets. All data referenced or analyzed in this article are available in the original published papers, which are cited accordingly. No new data were created in this study.

## Conflicts of interest

There are no conflicts to declare.

## Acknowledgements

This work was supported by the Shenzhen Science and Technology Innovation Committee (KCXFZ20201221173413038).

## References

- 1 A. Grubler, C. Wilson, N. Bento, B. Boza-Kiss, V. Krey, D. L. McCollum, N. D. Rao, K. Riahi, J. Rogelj, S. De Stercke, J. Cullen, S. Frank, O. Fricko, F. Guo, M. Gidden, P. Havlik, D. Huppmann, G. Kiesewetter, P. Rafaj, W. Schoepp and H. Valin, *Nat. Energy*, 2018, **3**, 515–527.
- 2 S. Mukhtarov, S. Yuksel and H. Dincer, *Renewable Energy*, 2022, **187**, 169–176.
- 3 A. Rode, T. Carleton, M. Delgado, M. Greenstone, T. Houser, S. Hsiang, A. Hultgren, A. Jina, R. E. Kopp, K. E. McCusker, I. Nath, J. Rising and J. Yuan, *Nature*, 2021, **598**, 308–314.
- 4 Y. Liu, K. Liu, P. Wang, Z. Jin and P. Li, *Carbon Neutrality*, 2023, **2**, 14.
- 5 M. R. Pratama, R. Muthia and W. W. Purwanto, *Carbon Neutrality*, 2023, **2**, 26.
- 6 C. Zhao, S. Ju, Y. Xue, T. Ren, Y. Ji and X. Chen, *Carbon Neutrality*, 2022, **1**, 7.
- 7 M. Farghali, A. I. Osman, I. M. A. Mohamed, Z. Chen, L. Chen, I. Ihara, P.-S. Yap and D. W. Rooney, *Environ. Chem. Lett.*, 2023, **21**, 2003–2039.
- 8 Y. Jing, Y. Guo, Q. Xia, X. Liu and Y. Wang, *Chem*, 2019, **5**, 2520–2546.
- 9 K. Lee, Y. Jing, Y. Wang and N. Yan, *Nat. Rev. Chem.*, 2022, **6**, 635–652.
- 10 Y. Liu, B. Ma, J. Tian and C. Zhao, *Sci. Adv.*, 2024, **10**, eadn0252.
- 11 Y. Yang, S. Yuan, H. Pan, Z. Li, X. Shen and Y. Gao, *Green Chem.*, 2023, **25**, 1004–1013.
- 12 P. Guo, S. Yuan, B. Guo, S. Li and Y. Gao, *Catal. Sci. Technol.*, 2023, **13**, 1128–1139.
- 13 X. Fang, R. Gong, D. Yang, C. Li, Y. Zhang, Y. Wang, G. Nie, M. Li, X. Peng and B. Zhang, *J. Am. Chem. Soc.*, 2024, **146**, 15251–15263.
- 14 J. Ma, Y. Yu, D. Chu, S. Zhu, Q. Liu and H. Yin, *J. Polym. Environ.*, 2024, **1**–10.
- 15 W. Deng, Y. Feng, J. Fu, H. Guo, Y. Guo, B. Han, Z. Jiang, L. Kong, C. Li, H. Liu, P. T. T. Nguyen, P. Ren, F. Wang, S. Wang, Y. Wang, Y. Wang, S. S. Wong, K. Yan, N. Yan, X. Yang, Y. Zhang, Z. Zhang, X. Zeng and H. Zhou, *Green Energy Environ.*, 2023, **8**, 10–114.
- 16 Y. Yue, X. Liu, M. Shakouri, Y. Hu, Y. Guo and Y. Wang, *Catal. Today*, 2024, **433**, 114688.
- 17 Z. Gao, B. Ma, S. Chen, J. Tian and C. Zhao, *Nat. Commun.*, 2022, **13**, 3343.
- 18 W. Deng, Y. Wang and N. Yan, *Curr. Opin. Green Sustainable Chem.*, 2016, **2**, 54–58.
- 19 L. Dong, Y. Wang, Y. Dong, Y. Zhang, M. Pan, X. Liu, X. Gu, M. Antonietti and Z. Chen, *Nat. Commun.*, 2023, **14**, 4996.
- 20 W. Deng, Y. Wang, S. Zhang, K. M. Gupta, M. J. Hülsey, H. Asakura, L. Liu, Y. Han, E. M. Karp and G. T. Beckham, *Proc. Natl. Acad. Sci. U. S. A.*, 2018, **115**, 5093–5098.
- 21 L. Li, Z. Guo, X. Liu, M. Shakouri, Y. Hu, Y. Guo and Y. Wang, *Carbon Neutrality*, 2024, **3**, 5.
- 22 Y. Gao, J. Zhang, X. Chen, D. Ma and N. Yan, *ChemPlusChem*, 2014, **79**, 825–834.
- 23 Y. Zhu, J. Qi, X. Li, X. Li, B. Ma, X. Zhang, J. Tian and C. Zhao, *ACS Catal.*, 2024, **14**, 13672–13683.
- 24 C.-H. Zhou, X. Xia, C.-X. Lin, D.-S. Tong and J. Beltramini, *Chem. Soc. Rev.*, 2011, **40**, 5588–5617.
- 25 H. Kobayashi, T. Sagawa and A. Fukuoka, *Chem. Commun.*, 2023, **59**, 6301–6313.
- 26 F. M. Kerton, Y. Liu, K. W. Omari and K. Hawboldt, *Green Chem.*, 2013, **15**, 860–871.
- 27 H. Amiri, M. Aghbashlo, M. Sharma, J. Gaffey, L. Manning, S. M. Moosavi Basri, J. F. Kennedy, V. K. Gupta and M. Tabatabaei, *Nat. Food*, 2022, **3**, 822–828.
- 28 S. Cao, Y. Liu, L. Shi, W. Zhu and H. Wang, *Green Chem.*, 2022, **24**, 493–509.
- 29 J. Dai, F. Li and X. Fu, *ChemSusChem*, 2020, **13**, 6498–6508.
- 30 N. Yan and X. Chen, *Nature*, 2015, **524**, 155–157.
- 31 X. Chen, S. Song, H. Li, G. Gözaydın and N. Yan, *Acc. Chem. Res.*, 2021, **54**, 1711–1722.
- 32 M. J. Hülsey, H. Yang and N. Yan, *ACS Sustainable Chem. Eng.*, 2018, **6**, 5694–5707.
- 33 X. Chen, B. Zhang, Y. Wang and N. Yan, *Chimia*, 2015, **69**, 120.
- 34 M. J. Hülsey, *Green Energy Environ.*, 2018, **3**, 318–327.
- 35 X. Chen, H. Yang and N. Yan, *Chem. – Eur. J.*, 2016, **22**, 13402–13421.
- 36 P. Beaney, J. Lizardi-Mendoza and M. Healy, *J. Chem. Technol. Biotechnol.*, 2005, **80**, 145–150.
- 37 A. Percot, C. Viton and A. Domard, *Biomacromolecules*, 2003, **4**, 12–18.
- 38 F. Shahidi and J. Synowiecki, *J. Agric. Food Chem.*, 1991, **39**, 1527–1532.
- 39 T. Setoguchi, T. Kato, K. Yamamoto and J.-I. Kadokawa, *Int. J. Biol. Macromol.*, 2012, **50**, 861–864.
- 40 H. Xie, S. Zhang and S. Li, *Green Chem.*, 2006, **8**, 630–633.
- 41 R. P. Swatloski, S. K. Spear, J. D. Holbrey and R. D. Rogers, *J. Am. Chem. Soc.*, 2002, **124**, 4974–4975.
- 42 F. Sedaghat, M. Yousefzadi, H. Toiserkani and S. Najafipour, *Int. J. Biol. Macromol.*, 2016, **82**, 279–283.
- 43 S. Duan, L. Li, Z. Zhuang, W. Wu, S. Hong and J. Zhou, *Carbohydr. Polym.*, 2012, **89**, 1283–1288.
- 44 W. L. Teng, E. Khor, T. K. Tan, L. Y. Lim and S. C. Tan, *Carbohydr. Res.*, 2001, **332**, 305–316.



- 45 H. Yang, G. Gözaydın, R. R. Nasaruddin, J. R. G. Har, X. Chen, X. Wang and N. Yan, *ACS Sustainable Chem. Eng.*, 2019, **7**, 5532–5542.
- 46 H. Kim, S. Kang, K. Li, D. Jung, K. Park and J. Lee, *Int. J. Biol. Macromol.*, 2021, **169**, 122–129.
- 47 M. Bisht, I. P. E. Macário, M. C. Neves, J. L. Pereira, S. Pandey, R. D. Rogers, J. A. P. Coutinho and S. P. M. Ventura, *ACS Sustainable Chem. Eng.*, 2021, **9**, 16073–16081.
- 48 X. Sun, Q. Wei, Y. Yang, Z. Xiao and X. Ren, *J. Environ. Chem. Eng.*, 2022, **10**, 106859.
- 49 P. S. Saravana, T. C. Ho, S.-J. Chae, Y.-J. Cho, J.-S. Park, H.-J. Lee and B.-S. Chun, *Carbohydr. Polym.*, 2018, **195**, 622–630.
- 50 J. Zhao, C. M. Pedersen, H. Chang, X. Hou, Y. Wang and Y. Qiao, *iScience*, 2023, **26**, 106980.
- 51 Z. Li, C. Liu, S. Hong, H. Lian, C. Mei, J. Lee, Q. Wu, M. A. Hubbe and M.-C. Li, *Chem. Eng. J.*, 2022, **446**, 136953.
- 52 P. Zhou, J. Li, T. Yan, X. Wang, J. Huang, Z. Kuang, M. Ye and M. Pan, *Carbohydr. Polym.*, 2019, **225**, 115255.
- 53 Y. Ma, Q. Xia, Y. Liu, W. Chen, S. Liu, Q. Wang, Y. Liu, J. Li and H. Yu, *ACS Omega*, 2019, **4**, 8539–8547.
- 54 M. Feng, X. Lu, J. Zhang, Y. Li, C. Shi, L. Lu and S. Zhang, *Green Chem.*, 2019, **21**, 87–98.
- 55 S. Hong, Y. Yuan, Q. Yang, P. Zhu and H. Lian, *Carbohydr. Polym.*, 2018, **201**, 211–217.
- 56 Y. Liu, C. Stähler, J. N. Murphy, B. J. Furlong and F. M. Kerton, *ACS Sustainable Chem. Eng.*, 2017, **5**, 4916–4922.
- 57 T. T. Pham, X. Chen, N. Yan and J. Sperry, *Monatsh. Chem.*, 2018, **149**, 857–861.
- 58 T. T. Pham, X. Chen, T. Söhnle, N. Yan and J. Sperry, *Green Chem.*, 2020, **22**, 1978–1984.
- 59 J. G. Pereira, J. M. J. M. Ravasco, J. R. Vale, F. Queda and R. F. A. Gomes, *Green Chem.*, 2022, **24**, 7131–7136.
- 60 T. T. Pham, A. C. Lindsay, S.-W. Kim, L. Persello, X. Chen, N. Yan and J. Sperry, *ChemistrySelect*, 2019, **4**, 10097–10099.
- 61 T. T. Pham, G. Gözaydın, T. Söhnle, N. Yan and J. Sperry, *Eur. J. Org. Chem.*, 2019, 1355–1360.
- 62 A. D. Sadiq, X. Chen, N. Yan and J. Sperry, *ChemSusChem*, 2018, **11**, 532–535.
- 63 K. W. Omari, L. Dodot and F. M. Kerton, *ChemSusChem*, 2012, **5**, 1767–1772.
- 64 M. W. Drover, K. W. Omari, J. N. Murphy and F. M. Kerton, *RSC Adv.*, 2012, **2**, 4642–4644.
- 65 X. Chen, S. L. Chew, F. M. Kerton and N. Yan, *Green Chem.*, 2014, **16**, 2204–2212.
- 66 X. Chen, Y. Liu, F. M. Kerton and N. Yan, *RSC Adv.*, 2015, **5**, 20073–20080.
- 67 X. Chen, Y. Gao, L. Wang, H. Chen and N. Yan, *ChemPlusChem*, 2015, **80**, 1565–1572.
- 68 D. Padovan, H. Kobayashi and A. Fukuoka, *ChemSusChem*, 2020, **13**, 3594–3598.
- 69 J. Wang, H. Zang, S. Jiao, K. Wang, Z. Shang, H. Li and J. Lou, *Sci. Total Environ.*, 2020, **710**, 136293.
- 70 H. Zang, Y. Feng, M. Zhang, K. Wang, Y. Du, Y. Lv, Z. Qin and Y. Xiao, *Carbohydr. Res.*, 2022, **522**, 108679.
- 71 H. Zang, H. Li, S. Jiao, J. Lou, Y. Du and N. Huang, *ChemistrySelect*, 2021, **6**, 3848–3857.
- 72 H. Zang, Y. Feng, J. Lou, K. Wang, C. Wu, Z. Liu and X. Zhu, *J. Mol. Liq.*, 2022, **366**, 120281.
- 73 K. Wang, Y. Xiao, C. Wu, Y. Feng, Z. Liu, X. Zhu and H. Zang, *Carbohydr. Res.*, 2023, **524**, 108742.
- 74 Y. Du, H. Zang, Y. Feng, K. Wang, Y. Lv and Z. Liu, *J. Mol. Liq.*, 2022, **347**, 117970.
- 75 K. Chen, C. Wu, C. Wang, A. Zhang, F. Cao and P. Ouyang, *Mol. Catal.*, 2021, **516**, 112001.
- 76 C. Wang, C. Wu, A. Zhang, K. Chen, F. Cao and P. Ouyang, *ChemistrySelect*, 2022, **7**, e202104574.
- 77 J. Zhao, C. M. Pedersen, H. Chang, X. Hou, Y. Wang and Y. Qiao, *iScience*, 2023, **26**, 106980.
- 78 X. Ji, J. Kou, G. Gözaydın and X. Chen, *Appl. Catal., B*, 2024, **342**, 123379.
- 79 M. Osada, H. Kobayashi, T. Miyazawa, S. Suenaga and M. Ogata, *Int. J. Biol. Macromol.*, 2019, **136**, 994–999.
- 80 M. Osada, K. Kikuta, K. Yoshida, K. Totani, M. Ogata and T. Usui, *Green Chem.*, 2013, **15**, 2960–2966.
- 81 M. Osada, S. Shoji, S. Suenaga and M. Ogata, *Fuel Process. Technol.*, 2019, **195**, 106154.
- 82 M. Osada, K. Kikuta, K. Yoshida, K. Totani, M. Ogata and T. Usui, *RSC Adv.*, 2014, **4**, 33651–33657.
- 83 C. H. M. van der Loo, M. L. G. Borst, K. Pouwer and A. J. Minnaard, *Org. Biomol. Chem.*, 2021, **19**, 10105–10111.
- 84 R. F. A. Gomes, B. M. F. Gonçalves, K. H. S. Andrade, B. B. Sousa, N. Maulide, G. J. L. Bernardes and C. A. M. Afonso, *Angew. Chem.*, 2023, e202304449.
- 85 C. Lin, H. Yang, X. Gao, Y. Zhuang, C. Feng, H. Wu, H. Gan, F. Cao, P. Wei and P. Ouyang, *ChemSusChem*, 2023, **16**, e202300133.
- 86 M. G. Davidson, S. Elgie, S. Parsons and T. J. Young, *Green Chem.*, 2021, **23**, 3154–3171.
- 87 J. Slak, B. Pomeroy, A. Kostyniuk, M. Grile and B. Likozar, *Chem. Eng. J.*, 2022, **429**, 132325.
- 88 X. Cai, Z. Wang, Y. Ye, D. Wang, Z. Zhang, Z. Zheng, Y. Liu and S. Li, *Renewable Sustainable Energy Rev.*, 2021, **150**, 111452.
- 89 J. Chakravarty and T. A. Edwards, *Energy Nexus*, 2022, **8**, 100149.
- 90 A. Jardine and S. Sayed, *Curr. Opin. Green Sustainable Chem.*, 2016, **2**, 34–39.
- 91 A. A. Rosatella, S. P. Simeonov, R. F. M. Frade and C. A. M. Afonso, *Green Chem.*, 2011, **13**, 754–793.
- 92 A. A. Turkin, E. V. Makshina and B. F. Sels, *ChemSusChem*, 2022, **15**, e202200412.
- 93 J. Liang, J. Jiang, T. Cai, C. Liu, J. Ye, X. Zeng and K. Wang, *Green Energy Environ.*, 2024, **9**, 1384–1406.
- 94 H. Wu, R. Zhang, Y. Zhai, X. Song, J. Xiong, X. Li, Y. Qiao, X. Lu and Z. Yu, *ChemSusChem*, 2023, **16**, e202201809.
- 95 L. Zhu, X. Fu, Y. Hu and C. Hu, *ChemSusChem*, 2020, **13**, 4812–4832.
- 96 M. E. Zakrzewska, E. Bogel-Lukasik and R. Bogel-Lukasik, *Chem. Rev.*, 2011, **111**, 397–417.
- 97 L. Lu, X. Ji, X. Wang, F. Jin and X. Chen, *Ind. Eng. Chem. Res.*, 2023, **62**, 11248–11257.
- 98 T. R. Zembower, G. A. Noskin, M. J. Postelnick, C. Nguyen and L. R. Peterson, *Int. J. Antimicrob. Agents*, 1998, **10**, 95–105.
- 99 A. Blanco and G. Blanco, in *Medical Biochemistry*, ed. A. Blanco and G. Blanco, Academic Press, 2017, pp. 73–97.
- 100 K. M. Vårum, M. H. Ottøy and O. Smidsrød, *Carbohydr. Polym.*, 2001, **46**, 89–98.
- 101 A. Einbu, H. Grasdalen and K. M. Vårum, *Carbohydr. Res.*, 2007, **342**, 1055–1062.
- 102 N. Kazami, M. Sakaguchi, D. Mizutani, T. Masuda, S. Wakita, F. Oyama, M. Kawakita and Y. Sugahara, *Carbohydr. Polym.*, 2015, **132**, 304–310.
- 103 Y. Pierson, X. Chen, F. D. Bobbink, J. Zhang and N. Yan, *ACS Sustainable Chem. Eng.*, 2014, **2**, 2081–2089.
- 104 J. Zhang and N. Yan, *Green Chem.*, 2016, **18**, 5050–5058.
- 105 J. Zhang and N. Yan, *ChemCatChem*, 2017, **9**, 2790–2796.
- 106 J. Cheng, A. Armugam, Y. Yang, F. Jin, Y. Zhang and N. Yan, *ChemSusChem*, 2023, **16**, e202300591.
- 107 N. Rodriguez Quiroz, A. M. D. Padmanathan, S. H. Mushrif and D. G. Vlachos, *ACS Catal.*, 2019, **9**, 10551–10561.
- 108 G. Gözaydın, S. Song and N. Yan, *Green Chem.*, 2020, **22**, 5096–5104.
- 109 G. Gözaydın, Q. Sun, M. Oh, S. Lee, M. Choi, Y. Liu and N. Yan, *ACS Sustainable Chem. Eng.*, 2023, **11**, 2511–2519.
- 110 Y. Wang, J. Kou, X. Wang and X. Chen, *Green Chem.*, 2023, **25**, 2596–2607.
- 111 G. Margoutidis, V. H. Parsons, C. S. Bottaro, N. Yan and F. M. Kerton, *ACS Sustainable Chem. Eng.*, 2018, **6**, 1662–1669.
- 112 M. Yabushita, H. Kobayashi, K. Kuroki, S. Ito and A. Fukuoka, *ChemSusChem*, 2015, **125**, 187–197.
- 113 D. De Chavez, H. Kobayashi, A. Fukuoka and J.-Y. Hasegawa, *J. Phys. Chem. A*, 2021, **125**, 187–197.
- 114 H. Kobayashi, Y. Suzuki, T. Sagawa, M. Saito and A. Fukuoka, *Angew. Chem., Int. Ed.*, 2023, **62**, e202214229.
- 115 X. Chen, H. Yang, Z. Zhong and N. Yan, *Green Chem.*, 2017, **19**, 2783–2792.
- 116 T. Di Nardo, C. Hadad, A. Nguyen Van Nhien and A. Moores, *Green Chem.*, 2019, **21**, 3276–3285.
- 117 X. Liu, S. Li, Y. Liu and Y. Cao, *Chin. J. Catal.*, 2015, **36**, 1461–1475.
- 118 J. Iglesias, I. Martínez-Salazar, P. Mairesles-Torres, D. Martín Alonso, R. Mariscal and M. López Granados, *Chem. Soc. Rev.*, 2020, **49**, 5704–5771.

- 119 A. T. Quitain, M. Faisal, K. Kang, H. Daimon and K. Fujie, *J. Hazard. Mater.*, 2002, **93**, 209–220.
- 120 Y. Fang, X. Zeng, P. Yan, Z. Jing and F. Jin, *Ind. Eng. Chem. Res.*, 2012, **51**, 4759–4763.
- 121 Z. Huo, Y. Fang, G. Yao, X. Zeng, D. Ren and F. Jin, *J. Energy Chem.*, 2015, **24**, 207–212.
- 122 X. Gao, X. Chen, J. Zhang, W. Guo, F. Jin and N. Yan, *ACS Sustainable Chem. Eng.*, 2016, **4**, 3912–3920.
- 123 M. Qi, X. Chen, H. Zhong, J. Wu and F. Jin, *ACS Sustainable Chem. Eng.*, 2020, **8**, 18661–18670.
- 124 J. Wu, M. Qi, G. Gözaydın, N. Yan, Y. Gao and X. Chen, *Ind. Eng. Chem. Res.*, 2021, **60**, 3239–3248.
- 125 B. L. Stocker and M. S. M. Timmer, *ChemBioChem*, 2013, **14**, 1164–1184.
- 126 J. Dai, G. Gözaydın, C. Hu and N. Yan, *ACS Sustainable Chem. Eng.*, 2019, **7**, 12399–12407.
- 127 Y. Ohmi, S. Nishimura and K. Ebitani, *ChemSusChem*, 2013, **6**, 2259–2262.
- 128 Y. Zheng, D. Xu, L. Zhang and X. Chen, *Chem. – Asian J.*, 2022, **17**, e202200556.
- 129 K. Techikawara, H. Kobayashi and A. Fukuoka, *ACS Sustainable Chem. Eng.*, 2018, **6**, 12411–12418.
- 130 J. Dai, Q. Cao, Z. Du, R. Yang, D. Yang, F. Li and X. Gu, *Catal. Commun.*, 2023, **185**, 106812.